Spring 2015

Interaction of gold nanomaterials with the edible food crop, Helianthus annuus (Common sunflower)

Meaghan Estelle Kern
University of Iowa

INTERACTION OF GOLD NANOMATERIALS WITH THE EDIBLE FOOD CROP, *HELIANTHUS ANNUUS*(COMMON SUNFLOWER)

by

Meaghan Estelle Kern

A thesis submitted in partial fulfillment of the requirements for the Master of Science degree in Civil and Environmental Engineering
in the Graduate College of
The University of Iowa

May 2015

Thesis Supervisor: Professor Jerald L. Schnoor

Graduate College
The University of Iowa
Iowa City, Iowa

CERTIFICATE OF APPROVAL

_____

MASTER'S THESIS

_____

This is to certify that the Master's thesis of

Meaghan Estelle Kern

has been approved by the Examining Committee
for the thesis requirement for the Master of Science
degree in Civil and Environmental Engineering at the May 2015
graduation.

Thesis Committee:_____
Jerald L. Schnoor, Thesis Supervisor

_____
Rich Valentine

_____
David Peate

ACKNOWLEDGEMENTS

I would like to thank my advisor Jerry Schnoor for allowing me this opportunity to come here as well as providing the grants and supports to fund me. I would like to thank Guangshu Zhai and Nastaran Moradi for their help and direction during my research, and Kathy Walters who graciously walked me through the TEM process and helped me understand the images. I also thank Dr. David Peate for patiently assisting me during my time prepping, measuring, and analyzing my samples with the ICP-MS. Finally, I would like to thank my family and friends for supporting me during my time here at The University of Iowa. I would especially like to thank my mom, Marriah Kern, Melanie Kern-Kuhn, and Melissa Karo.

PUBLIC ABSTRACT

By the year 2020, the nanotechnology market is expected to be three trillion dollars. With a quasi-exponential increase in consumer products, which contain nanomaterials, there is likely to be an equal increase in nanoparticles entering the environment. As a result, it is imperative to fully understand the relationship between nanomaterials and the food chain, including plants.

In this study, the relationship between gold nanomaterials and the edible food crop, *Helianthus annuus* was investigated. First, an attempt to inhibit the uptake of nanoparticles into the roots of *H. annuus* was investigated by decreasing temperature. Second, the interactions between citrate-stabilized 20 nm diameter Au nanoparticles and sunflower seedlings were explored by exposing sunflower to a range of concentrations (3.0-40.0 mg/L). Nanoparticle sorption to roots was estimated using a linear isotherm with a distribution coefficient, Kd. Finally, sunflowers were exposed to 20 nm Au nanoparticles and 25x69 nm CTAB-stabilized Au nanorods. Results showed there was no change in biomass growth and transpiration between sunflowers that were exposed to nanoparticles and the unexposed controls. Thus Au gold nanoparticles (20 nm) were shown to have no phytostimulatory or phytotoxic effect on sunflower seedlings during eight to ten day exposure experiments. However, 25x69 nm gold nanorods were phytotoxic to sunflowers at 6.0 mg/L, indicating a potential charge or chemical effect of the surface coating of the nanorods compared to the spherical gold nanoparticles

SCIENTIFIC ABSTRACT

By the year 2020, the nanotechnology market is expected to be three trillion dollars. Inevitably, these man-made materials will accumulate in the environment and it is imperative to fully understand the relationship between nanomaterials and the food chain, including plants.

In this study, the relationship between gold nanomaterials and the edible food crop, *Helianthus annuus* were investigated. First, an attempt to inhibit endocytosis and uptake into *H. annuus* root cells was investigated by decreasing temperature. Second, the interactions between citrate-stabilized 20 nm diameter Au nanoparticles and sunflower seedlings were explored by exposing sunflower seedlings to a range of concentrations (3.0-40.0 mg/L). Nanoparticle sorption to roots was estimated through the calculation of a distribution coefficient, Kd. The Kd value was approximately 900 mL/g. Membrane uptake efficiency was estimated as 10-17%. Overall, Au gold nanoparticles (20 nm) were shown to have no phytostimulatory or phytotoxic effect on sunflower seedlings during eight to ten day exposure experiments. However, 25x69 nm gold nanorods were phytotoxic to sunflowers at 6.0 mg/L, indicating a toxic effect from the surface coating of the nanorods compared to the spherical gold nanoparticles.

TABLE OF CONTENTS

LIST OF TABLES

TABLE OF FIGURES

Chapter 1 Introduction and Objectives

1.1 Introduction

Engineered nanomaterials (ENM's) are used in many industries throughout the world. They are defined as material that measures between 4-100 nm and are specifically engineered for a desired application (Arruda, Silva, Galazzi, Azevedo, & Arruda, 2015). For comparison, a DNA molecule is 2.5 nm wide, a protein is approximately 50 nm, and a flu virus is 100 nm(Thakkar, Mhatre, & Parikh, 2010). The extremely small size of nanomaterials is why they may have exceptional mechanical, chemical catalytic, and/or optical properties that differ from their bulk material. The large surface area at the nano-scale level is what may increase their biological/chemical activity, and as a result, increased usefulness. As a result of their unique properties, the demand to engineer and create more engineered nanomaterials has exploded over the last decade. According to the Consumer Products Inventory completed by the Project on Emerging Nanotechnologies (PEN) there are over 1600 manufacturer-identified nanomaterial-based products in the consumer market (PEN, 2015).

There are ENM's of all shapes and sizes. For examples, there are carbonaceous nanomaterials, zero valent metals such as iron, gold, and silver, nano-inorganic particles and nanopolymers. From these nanomaterials, nanoproducts with various surface structures and different chemical coatings are being created into the form of nanoparticles (NPs), nanotubes, nanosheets and nanofibers (Klaine et al., 2008). Their multifunctional capability allows them to be used in technology, biomedicine, food, agriculture, as well as many commercial product applications.

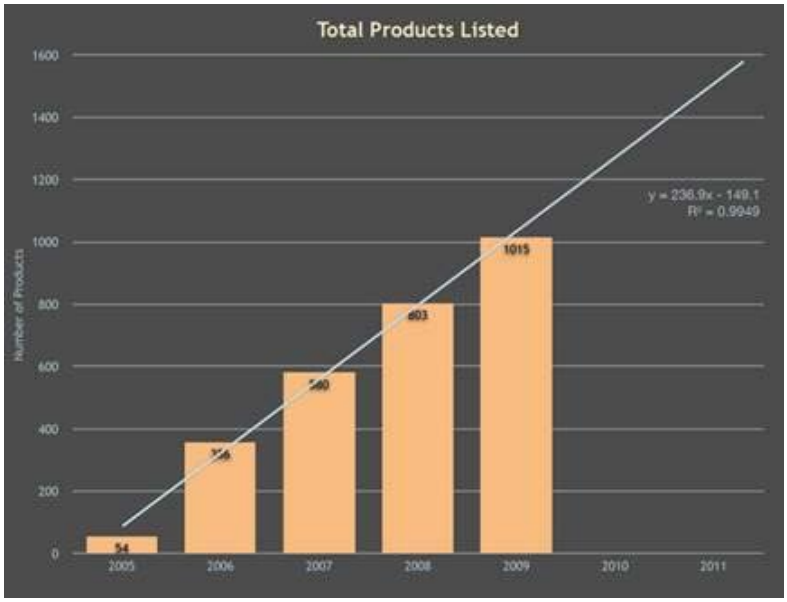

Figure 1-1: Linear progression of commercially available NM's according to the Project on Environmental Nanomaterials (PEN). Taken From (Kuiken, 2009).

Nanomaterial forms and functions are expected to increase dramatically and their uses are expected to impact every industry that uses materials (Figure 1-1). The National Nanotechnology Initiative was created in 1999 as a collective knowledge source to advance, understand and promote further research in this industry. This nanotechnology industry is still rapidly evolving. In 2009, the estimated worldwide market for nanotechnology was $250 billion dollars, and $91 billion were US products, which incorporates nanoscale materials. By 2020, the increased integration of nanoscience and engineering will lead to a variety of new applications expected to be equal to $3 trillion in the U.S.

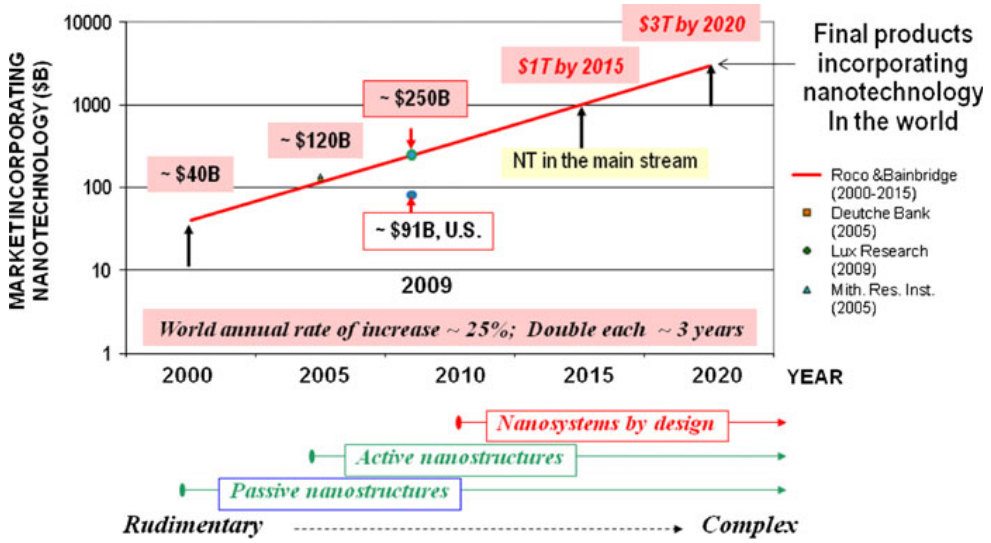

Figure 1-2: Expected World Market Value of Nanotechnology in 2020. Taken from(Roco, 2011).

Figure 1-2 shows the estimated global market value of nanomaterials as $3 trillion by 2020. The rate of nanomaterial technology is considered to be quasi-exponential, growing at a rate of 25-35 % annually (Roco, 2011). It is suggested that nanomaterial based consumer products are growing faster than we are able to fully understand their health effects and environmental impacts (Ranjan, 2014).

One industry that is expected to exponentially grow from nanotechnology is the food and agriculture industry with new products, processing and nutritional aspects. Currently, agricultural researchers are looking at using nanoparticles as novel pesticides, targeted gene delivery vehicles, agrochemical delivery, and as sensors to monitor soil quality (Ranjan, 2014). Other potential applications that merge biotechnology, nanotechnology and agriculture are: nanoscale vehicles for effective delivery of micronutrients and sensitive bioactive, re-engineering of crops at the genetic and cellular level, and development of nano-based foods that have less salt, fat, and sugar while

retaining texture and taste. The convergence of biotechnology, agriculture and nanotechnology are considered to be a priority due to the need to feed a world population of 9 billion by 2050 (Chen, Seiber, & Hotze, 2014). The increased commercialization of nanoparticles, especially within the food and agriculture industry has created three dichotomies when looking at the relationship between nanoparticles and plants. One mode of thinking is that nanoparticles can be used to enhance the growth and yield of crops. Crops can be stimulated with nanomaterials to have larger and faster commercial yield, and nanomaterials can have targeted gene delivery for key traits or for treatment of diseases. Nanomaterials are now considered as one of the premier candidates to accurately deliver drugs and key proteins to a targeted organ in mammals. Researchers are also hoping to deliver nanoparticles and medicines to key plant organs which are most commonly affected by pathogens (Corredor et al., 2009) (Deng, White, & Xing, 2014; Gonzalez-Melendi et al., 2008).

On the opposite side of the spectrum is the idea that the more man-made nanoparticles, the greater the hazard of accumulation in ecosystems, natural waters and crops. The fate of these nanomaterials and their relationship with the environment is still not clear and nanomaterials are often viewed as emerging pollutants. As a result of the increased use of nanomaterials in products, it is vital to learn their fate in the environment as well as the specific interactions with plants, the base of the food chain. Engineered nanomaterials persist in the environment, similar to natural nanoparticles (Deng et al., 2014). As a result, ENM's have the ability to interact with plant species in three different ways: water, soil, and air. Nanoparticles can persist through the wastewater treatment process and be discharged to receiving streams, and are easily

transported via air emissions and deposited to topsoil. According to the National Research Committee, 60% of biosolids are applied to agricultural fields and these biosolids (digested, dewatered sewage sludge) may also contain nanomaterials (Deng et al., 2014). Nanoparticles persist through water and wastewater treatment and the presence of concentrated nanoparticles in biosolids has the potential to cause toxic effects to plants and animal species. Coastal areas and estuaries are expected to be a sink for nanoparticles due to agriculture run-off, air deposits and wastewater treatment effluent. Animals within these ecosystems may be at risk. For example, bivalve mollusks have been shown to have immune responses to various types of nanoparticles (Canesi et al., 2012). Also, studies have shown evidence of the biomagnification of gold nanoparticles throughout the food chain (Judy, Unrine, & Bertsch, 2010).

The third approach to understanding plants and the environment is using plants in order to clean up the aggregated nanoparticles in the environment through various forms of phytoremediation (phytostabilization, phytoextraction and/or phytomining). Phytoremediation is a general term used to describe different ways plants can be used to clean soil and groundwater for the benefit of the ecosystem. One type of phytoremediation is phytostabilization, where plants are used to immobilize metals because the metals actively sorb to the roots and/or the plants transpire large amounts of water from the root zone helping to exert hydraulic control on the downward migration of contaminants. Phytoextraction is a term used to describe the metal uptake and translocation of metals into the plant biomass and the toxic metal will no longer exist in the soil. Finally phytomining is phytoextraction of the metal from soil, then harvesting that plant and smelting the metal commodity out of the plant for reuse. Leaf extracts have

been shown to produce nanoparticles by reduction of metal ions through organic compounds such as proteins, polyphenols and carbohydrates (Kumar & Yadav, 2009). Phytomining is the process of phytoextraction then harvest the biomass to extract the nanomaterials. For instance, Mahmood and authors have shown that water hyacinth (*Eichhronia crassipes*) are able to uptake and translocate metals from the soil into the plant biomass. The plant biomass can then be smelted and converted into ENM's. The plant is used as the tool to retrieve the commodity from the ground and harvested to retrieve and sell the nanomaterials (Mahmood, 2012). There have been studies that have shown promise for plants to sorb and translocate certain nanoparticles into above ground biomass, especially metal-based nanoparticles. Wilson-Corral and associates discovered that gold could accumulate in *H. annuus*, even though gold is not known to be bioavailable to plants. They found that sunflower bioaccumulated gold in field studies with addition of solubilizing agents (NaCN, NH_4SCN and $(NH_4)_2S_2O_3$) to have a maximum gold concentration of 21.3, 3.50, 1.64 mg/kg in roots, shoots, and leaves respectively (Wilson-Corral, 2010). Since gold nanoparticles have different functional properties than larger gold particles in the solid state, gold nanoparticles can potentially be more bioavailable to plants. In order to understand nanoparticle interaction with plants, it is important to first study their sorption and bioavailability.

Overall, it is vital to understand the relationship between nanomaterials and plants because so much is unknown. Is there a toxicological effect exerted by nanoparticles on plants? Is there biomagnification of nanomaterials through the food chain? Could nanoparticles harm human health through consumption of edible food crops? Can plants help us cleanup water or soil, or prevent further pollution of water and

crops as part of a treatment technology? If there is not an environmental or human risk, can nanomaterials be used to improve and advance the agriculture industry? Finding an answer to some of these questions could help enlighten the relationship between nanomaterials and plants.

For this experiment, *Helianthus annuus* (common sunflower) was used. It is a popular annual species that is a human food and oil crop, as well as an ornamental plant and important food source for birds. It is a broad leaf species that is known to be a hyper-accumulator of metals(Seth, Misra, Singh, & Zolla, 2011). *H. annuus* (Sunflower*)* was a good candidate for this experiment because it is a food crop and because there is little previous research on sunflower and nanoparticles. Seedlings were used to accommodate the small hydroponic experiments in the laboratory. In addition, sunflowers are known to be a hardy plant that can withstand stress and low temperatures. Gold nanomaterials were used for this study because they are known to have strong electric fields (electron dense) on the surface that can be distinguishable within cells using transmission electron microscopy (TEM).

1.2 Goals and Objectives

1.2.1 Goals: The overall goals of this research was to study an important food plant system exposed to nanoparticles and to better understand how nanoparticles may enter into the plant seedlings, and where these man-made materials might accumulate within the plant system. A hydroponic plant system was studied by exposing plant roots to gold nanomaterials and by collecting transpiration data, overall biomass, and gold concentrations in solution. Gold concentrations within the plant tissue and solutions help us to understand if nanoparticles are uptaken and translocated within plant tissues-this was studied by Transmission Electron Microscopy (TEM) and Inductively Coupled Plasma Mass Spectroscopy (ICP-MS). In addition, estimating the sorption and speciation of gold nanoparticles of roots will provide a better understanding of the interaction between nanoparticles and this important commodity crop, sunflower.

1.2.2 Specific Objectives:

1. To determine if nanoparticle uptake by *H. annuus* can be completely inhibited by cold.
2. To study if phytotoxicity or phytostimulation occurs when *H. annuus* is exposed to gold nanoparticles (20 nm).
3. To determine if nanoparticles enter inside *H. annuus* root tissue and not just sorb to the outside of roots.
4. To ascertain if nanoparticles can translocate within the plants from roots to leaves to a measurable extent.

5. To determine equilibrium (4-hour) sorption values of gold nanoparticles onto the root of *H. annuus*.
6. To delineate the effect of surface charge of the nanoparticle when *H. annuus* is exposed to either 25x69 nm nanorods or 20 nm gold nanoparticles (average size, spherical shape) with different surface coatings and charge.

1.2.3 Specific H_o Hypothesis

1. Temperature will not have a significant impact on nanoparticle uptake because uptake of nanomaterials into roots is not via endocytosis. Endocytosis is known to be blocked at low temperatures because membrane fluidity is decreased (E. Etxeberria, Pozueta-Romero, J. Fernandez, E., 2012).
2. *H. annuus* will exhibit no statistically significant phytostimulation or phytotoxic effect compared to the controls when exposed to 20 nm gold nanoparticles because gold particles are relatively inert and non-reactive.
3. There will not be a statistically significant uptake or translocation of NPs into the vascular system of roots, shoots and leaves of *H. annuus* because AuNPs are not a required nutrient and not actively uptaken.
4. There will be no statistically significant difference (p-value≤ 0.05) in growth of *H. annuus* when plants are inoculated with similar concentration of gold nanorods versus gold nanoparticles.
5. Sorption to the root tissues will follow a classic Langmuir Isotherm based on attractive forces between nanoparticles and roots.

1.2.4 Tasks/Experiments

To study the specific objectives, five different experiments were performed and statistical significance was considered as a significance (p-value) less than or equal to 0.05.

Experiment 1-Effect of Temperature: *H. annuus* seeds were germinated, transplanted and inoculated with 3.0 mg/L of 20 nm gold nanoparticles (average diameter). Transpiration, biomass, and TEM images were used to compare the difference in uptake between those placed in a freezer set at 7.5 °C versus those *H. annuus* samples placed in a growth chamber at 25 ± 1 °C.

Experiment 2-Uptake and Translocation: *H. annuus* seeds were germinated, transplanted and inoculated with 10.0 mg/L and 14.0 mg/L of gold nanoparticles. Transpiration, biomass, TEM imaging, and ICP-MS measurements were undertaken in order to understand the uptake and translocation when *H. annuus* seeds were inoculated with gold nanoparticles.

Experiment 3-Concentration Dependency: To replicate experiment 2 and further understand the NP uptake and translocation. Three concentrations were used 4.0 mg/L, 10.0 mg/L and 40.0 mg/L to determine if results were similar to experiments 1 and 2 and to compare three different concentrations.

Experiment 4-Nanorods vs. Nanoparticle Toxicity to Sunflower: Plants used in this experiment were germinated from experiment 3. The purpose was to compare a

nanomaterial that was known to be phytotoxic to maize (Au nanorods) and to determine if it is also phytotoxic to sunflower.

Experiment 5- Sorption Isotherm for AuNPs to Roots: Roots utilized in this experiment were taken from seedlings germinated and grown in Experiment 3. Sunflower seedlings were allowed to grow in test tubes after germination for nine days. On the 9th day, roots were cut from the plants and placed into a new test tube in order to measure sorption of NPs onto roots. This was done by putting roots in four different concentrations of 20 nm Au NPs (2.0, 5.0, 10.0, 15.0 mg/L) for four hours on a shaker at 80 rpm. After four hours, solutions and roots were prepared for ICP-MS. This allows the estimation of a Kd value, the distribution coefficient between roots and solution containing nanoparticles.

Chapter 2 Literature Review

The main barriers that nanomaterials encounter when traversing through plant tissues are the cell wall and the cell membrane. This literature review describes the previous research that has been conducted to understand nanomaterials relationship with plants and how such materials can bypass a plant's line of defense. In addition, this literature review will examine the current research in the food and agricultural industry on nanomaterials. Finally the literature review will touch on the production of gold nanoparticles and gold nanorods and their applications.

2.1 Plant Cell Wall

There is a lot of uncertainty on the mechanism by which nanoparticles get in to plants. Plant cells consist of a cell wall and a cell membrane as their main barriers of protection. The cellulose cell wall is a meshwork of polymers. The primary cell wall is flexible and dynamic consortium of fibers. The secondary cell wall is considered to be less porous, due to densely packed crystalline cellulose microfibrils (Albersheim, 2011). Explicit research on the pore size has varied over the years. The variations are due to advancements in technology and various procedures used. For instance, Carpita and associates did one of the oldest cited experiments looking at cell size. They tried to measure the cell wall pore size of living plant cells and estimated the pore size framework for the primary cell wall as 3.5-5.2 nm (Carpita, 1979). Years later, researchers proposed that plant cells for that study were in hypertonic solution and propose the pore size range

of 4-9.2 nm (Albersheim, 2011). Other developments within electron microscopy and pectin research have made even larger pore size estimations of the primary cell wall to be 10 nm and a maximum of 20 nm. In addition, upon ice etching away the pectin's between the cell wall, pore sizes increased to 30-40 nm and a maximum of 60 nm (McCann, 1990). According to the research, the plant cell wall pore size suggests that nanomaterials should not be able to get in. NPs have an increased surface area to mass ratio and are believed to be highly reactive to their surroundings. This has suggested to cause an increase in activity with the cell wall and cell membrane (Rico, Majumdar, Duarte-Gardea, Peralta-Videa, & Gardea-Torresdey, 2011). Some research suggests that the increased activity could also be what prohibits NPs from entering the cell. Proseus and Boyer found only a small fraction of gold NPs penetrate through the cell wall of algal cells because of its high sorption capabilities (Proseus & Boyer, 2005). Despite the high sorption, research of various nanomaterials with a variety of plant species has continuously shown that nanomaterials are able to get through the plants first line of defense, the cell wall and accumulate in plant tissue. For instance, $C_6(OH)_{20}$ with a diameter less than 24 nm was found in *A. cepa* cells, but hydrophobic fullerenes C_{70} (18.2-100 nm) accumulated between the cell membrane and the cell wall. This contrast suggests that NPs are able to bypass cell wall pores, independent of size, but the characteristics of the NP can affect its permeability with the cell membrane. ENM's ability to bypass the cell wall despite being larger than the estimated pore size are thought to induce formation of larger pores, ultimately facilitating ENP uptake (Navarro et al., 2008). Another theory is that the ENM's which aggregate at the cell wall are able to increase permeability by damaging the cell

structure(Miralles, Church, & Harris, 2012). ENPs such as MWCNT's have been shown to just puncture the cell wall and cell membrane and enter (Wild & Jones, 2009).

2.2 Mechanisms of Plant Cell Uptake Through the Membrane

The plant cell membrane is selectively permeable. Small nonpolar ions can readily diffuse across the membrane. While on the other hand polar molecules, ions and exotic particles cannot easily permeate through the phospholipid bilayer. It has been thought that uptake mechanisms commonly found in mammalian cells were not possible in plant cells because of the turgor pressure from the cell wall. (E. Etxeberria, Pozueta-Romero, J. Fernandez, E., 2012) Recently, however, research has shown that nanoparticles are able to pass through the plasma membrane. Majority of studies on cell membrane uptake mechanisms have been conducted on mammalian cells and show nanoparticle uptake is selective. (Verma & Stellacci, 2010) There is limited research on plant uptake mechanisms, but current studies have shown plant cells are also selective.

It has been suggested that the cell membrane is selective based on the following nanoparticle characteristics: size, type, chemical composition, functionalization, and the local environment (Rico et al., 2011). In the review focusing on the cell membrane barrier, it is important to distinguish what type of plant model was used. Protoplasts are common plant models with the cell wall enzymatically removed, and this plant model is known to not represent realistic conditions (Liu, 2009). For this reason, a protoplast was decided against and a real model plant using a hydroponic system was proposed for this experiment. A hydroponic system is a simplified model system that allows for homogenous mixing and can be used to further distinguish the relationship between

nanoparticles and plants (Deng et al., 2014). Sunflowers are known to successfully grow in hydroponic conditions and were chosen for this experiment because there is no known research concerning the relationship between sunflowers and nanoparticles.

2.2.1 Endocytosis

The first key theory of how nanomaterials enter plants is endocytosis. Endocytosis is the uptake of extracellular materials through invagination of the plasma membrane. This process is well understood in mammalian cells, but in plant cells, the mechanism is not as clear. The tools for studying the mechanisms are restricted because plants have a cell wall and the staining procedures are limited to membrane-permeable dyes (Torney, Trewyn, Lin, & Wang, 2007). Oxidized single walled carbon nanotubes (SWCNT), less than 500 nm in length, were successfully found to traverse *Nicotiana tobacum* (cultivated tobacco) plant cells. Fluidic phase endocytosis was the suggested mechanism because nanotube uptake was significantly decreased upon treatment with known fluid phase endocytosis inhibitors. One of the main fluidic phase inhibitor used in this study was a temperature inhibitor. Endocytosis was suggested to be inhibited at a temperature of 4°C (Liu, 2009). Another experiment suggests two different endocytosis mechanisms for the uptake of two different nanoparticles. (E. Etxeberria, Gonzalez, & Pozueta, 2009) Protoplasts of *Acer psuedoplatunus* (sycamore maple) were incubated in a sucrose medium with fluorescent polystyrene carboxylate-modified nanospheres (40 nm). In addition, sycamore protoplasts were incubated with derivatized polyacylcrylic acid (PEG-coated) Cd/Se core and Zn/S shell quantum dots (20 nm). The 40 nm carboxylate-modified nanospheres incubated in a sucrose medium were commonly found in the vacuoles and outside several cells. In contrast, 20 nm quantum dots were found in large

cytosolic spherical organelles. The "trapping" of the QD's in vesicles is indicative of clathrin-independent endocytosis, while the polystyrene nano-spheres (40 nm) with sucrose stimulation is indicative of a distinctly different endocytic process (E. G. Etxeberria, P. , 2006). Clathrin-independent or fluid phase endocytosis is defined as the uptake of extracellular space that does not require binding of a specific ligand to a plasma membrane localized receptor. Capacity measurements of the clathrin-independent structures such as the "trapping vesicles" described are suggested to be 70-120 nm.(E. Etxeberria, Pozueta-Romero, J. Fernandez, E., 2012) Fluid-phase endocytosis was the suggested mechanism for uptake of the oxidized-SWCNT and for the PEG-coated CdSe/ZnS QD's (20 nm). In contrast, the carboxylate nanospheres (40 nm) resulted in accumulation in the vacuoles. This resulting location is known to be an indicator of receptor-mediated endocytosis. Receptor-mediated endocytosis is defined as the uptake of extracellular space, mediated by ligand binding and plasma membrane localized receptors (Rubbo S.D.; Russinova, 2012). Recently, research has shown the mechanistic pathway of receptor-mediated endocytosis where the receptor-ligand coupling with the marker present with in the vacuole (Irani NG, 2012). This final destination is the similar destination to the carboxylate nanospheres (40 nm) (E. G. Etxeberria, P. , 2006).

Two different endocytic mechanisms were also suggested after charged nanogold particles were used as a tool to illuminate endocytic pathways. It was found that positive charged nanogold had a higher affinity for the negatively charged cell membrane. Despite the decreased attraction, negative charged nanogold was still found within the plant cell. It was found that the negatively charged nanogold accumulated in different vesicles when compared to the positively charged nanogold (Onelli, Prescianotto-Baschong, Caccianiga,

& Moscatelli, 2008). Although they were unable to specifically distinguish the two different pathways, they theorized two different uptake pathways based on accumulation of the nanogold in two different locations. These results correlate with mammalian studies; in mammalian cells, research suggests a decreased rate of endocytosis with negatively charged nanoparticles, and nanoparticles with a positive charge rapidly internalized via a clathrin-dependent pathway. In addition, upon inhibition, more cationic particles than anionic cells transferred into mammalian cell.(Verma & Stellacci, 2010) This research provides evidence that nanoparticle uptake depends on different nanoparticle characteristics. Two different endocytic mechanisms (clathrin-dependent and clathrin-independent) are suggested mechanisms by which nanoparticles are able to traverse the cell membrane.

2.2.2 Non-specified Endocytosis Mechanisms/Stomata Foliar Pathway

Mesoporous silica nanoparticles (MSN's) are popular in vivo delivery system for mammalian cells, however, not widely used as nano-carriers for plant cells.(Xia et al., 2013) MSN's (approximately 200 nm), functionalized with triethylene glycol (TEG), and were taken into the cell via endocytosis mechanisms in tobacco mesophyll protoplasts. Non-functionalized MSN's (approximately 200 nm) were described as blocked from uptake.(Torney et al., 2007) However, non-functionalized ultra-fine MSN's (size 5-15 nm) in *Liriodendron* hybrid suspension cells were able to pass through the cell wall and membrane via cellular endocytosis.(Xia et al., 2013) Endocytosis was also the main theory because SWNT's were found in "endocytosis like" vesicles and these results are similar to mammalian cell studies.(Shen, Zhang, Li, Bi, & Yao, 2010) Plant uptake in sucrose-coated (+) TiO_2-NC with diameters of 2.8 ± 1.4 nm of Arabidopsis thaliana (thale cress) leaves

was studied. They found subcellular distribution of the sucrose-coated nanoconjugates and believe this is a result of endocytosis and stomata foliar uptake pathways.(Kurepa et al., 2010) Another study suggests stomata pathways for the uptake of fluorescent polystyrene particles with carboxylate-modified surfaces (43 ± 6 nm) into *Vicia faba* (field bean) epidermal cells (Eichert, Kurtz, Steiner, & Goldbach, 2008).

2.2.3 Non-endocytosis pathways

Other potential pathways that have been proposed are aquaporins. (Rico et al., 2011) Aquaporins are protein channels that selectively uptake water and potentially other important molecules for the cell. The suggested aquaporin cell size is 0.2-0.25 nm.(Tyerman, Niemietz, & Bramley, 2002). However some research has suggested that nanoparticles can cause the enlargement of these pores in order to increase water uptake that could allow for nanoparticles to sneak through (Rico et al., 2011). Specifically, multiple-walled carbon nanotubes (MWCNT's) have shown to cause enlargement of pores via gene expression of the water channel gene (NtPIP1) and the increased production of the corresponding protein (NtPIP1)(Khodakovskaya M.; de Silva M.; Biris, 2012). No specific research has suggested that aquaporin uptake is the main mechanism for nanoparticle uptake. However, C_{70} fullerenes were shown to enter rice plant cells and the osmotic pressure and capillary forces are the suggested method of uptake; and this could be related to aquaporin uptake (S. Lin et al., 2009). Large MWCNT's were shown to directly penetrate the cell wall and the cell membrane of wheat roots, however full uptake was never complete (Wild & Jones, 2009). MWCNT's less than 100 nm were shown to skip endosomal processing and directly enter *Catharanthus roseus* (Madagascar rosy periwinkle) protoplasts (Serag & Kaji, 2011). Other mechanisms have been tested on

mammalian cells and nanoparticle uptake, but not on plant cells. The following mechanisms are a result of different nanoparticle surface properties. Different nanoparticle surface properties could include various surface ligands and their corresponding interactions with the cell membrane. One potential mechanism based on the ligand-membrane interaction is snorkeling (Verma et al., 2008).

2.3 Nanoparticle Toxicity Studies

Regarding food and agriculture, there have been numerous studies that have used nanoparticles in order to study their effects on plants. As nanoparticles become more prevalent in the environment, it is necessary to understand the implications on humans and agriculture if plants contain nanoparticles. Therefore, there have been many studies using various types of plant species and nanomaterials to measure nanomaterial uptake, translocation and overall toxicity(Hawthorne, Musante, Sinha, & White, 2012; Larue et al., 2012; Rico et al., 2011). Current research has indicated that uptake, translocation and accumulation of nanomaterials in plants depend on the size, shape, functionalization, material, and stability of the nanomaterial as well as the plant species (Rico et al., 2011). In general, been there has been no conclusive trend between toxicity and food crops. However, plant toxicity from nanoparticles does appear to be a function of many factors including: nanoparticle concentration, size, functionalization or surface coating of the NPs, the plant species, life cycle stage, age of the plants, growth media, and dilution agent (Keller, 2010). Some research has suggested that nanoparticles can have a stimulatory effect on the growth of plants known as phytostimulation. *Arabidopsis thaliana* and *Populus deltoids x nigra* were found to be stimulated at low concentrations by PEG-coated 5 and 10 nm AgNPs and carbon-coated AgNPs (Wang et al., 2013). MWCNTs (5-50 µg/L)

were shown to enhance seed germination of tobacco cell cultures (Khodakovskaya, de Silva, Biris, Dervishi, & Villagarcia, 2012). TiO_2 NPs in soil 2.5 g- 40-g/kg soils were shown to improve the growth of spinach by enhancing photosynthesis and nitrogen-fixation(Zhang & Akbulut, 2011). Nano zero-valent iron was shown to trigger increased H^+-ATPase activity in *Arabidopsis thaliana*. This increased activity led to a wider stomata opening which could allow increase uptake of CO_2 (Kim, Oh, Yoon, Hwang, & Chang, 2015). Research has shown that plants have also been inhibited by exposure to nanoparticles. For instance, Zn NPs and ZnO NPs exposed to radish (*Raphanus sativus)*, rape (*Brassica napus*) and ryegrass (*Lolium perenne*) had significant effects on seed germination and root growth (D. Lin & Xing, 2007). For metal nanoparticles, Lee and associates show that mung bean (*Phaseolus radiatus*) and wheat (*Triticum aestivum*) with exposure to copper nanoparticles were phytotoxic. They showed that mung bean was more susceptible to toxic effects than wheat. They attributed the sensitivity of mung bean as a result of the root architecture. Mung bean is a dicot with one primary and multiple smaller roots while wheat, a monocot, does not have a primary root(Lee, 2008). This suggests that plants with a primary root may be more susceptible to toxic effects.

Other research results are mixed and show no effect, stimulatory or inhibitory effects, on plants. TiO_2 NPs were found to no impact on transpiration of willow tree cuttings in hydroponic solution. ((Seeger, Baun, Kästner, & Trapp, 2008). Various sizes of TiO_2 (14 nm to 655 nm) NPs were exposed to wheat (*T. aestivum*) and no change in biomass, transpiration and photosynthesis was observed (Larue et al., 2012).

2.4 Sunflower

Currently there has been little research on the relationship between nanoparticles and their uptake by sunflowers . Sunflowers, however, are known to be phytoaccumulators of metals (Singh & Sinha, 2004). Thus, it becomes important to understand the relationship between nanomaterials and ability of sunflowers to uptake, translocate and accumulate metals into its seed. According to the National Sunflower Association Industry report, approximately 2,399,910 lbs. of seed is produced for the purpose of producing sunflower oil. This accounts for 86.2% of the total crop ("Sunflower Statistics," 2015). It is important to understand the toxicity of nanoparticles to sunflower and if the manufacturing process of sunflower oil can diminish or enhance the toxicity. Furthermore, little research has been performed on the effects of plants of two well-known types of nanomaterials, gold nanoparticles versus gold nanorods.

2.5 Gold Nanoparticles Production and Applications

Gold nanoparticles are man-made materials that consist of an inorganic core that can be surrounded with an organic monolayer. The synthesis of modern gold nanoparticles dates to back to over 150 years ago (Faraday, 1857). Turkevich created the best known process for gold nanoparticle synthesis with associates in the 1950's.Turkevich studied various solutions to nucleate gold, and he found that spherical gold nanoparticles could be created in water through the reduction of hot chloroauric acid with small amounts of sodium citrate solution. The sodium citrate provides a reducing agent as well as a capping agent (Enustun & Turkevich, 1963). The current

method used to synthesize gold nanoparticles is through a seeding method which reduces new nucleation and allows the current nucleated AuNP to increase in size due to a surface catalyzed reduction of Au^{3+} by sodium citrate (Bastus, Comenge, & Puntes, 2011). Gold nanoparticles are commonly used in the biomedical industry. In the study, citrate stabilized gold nanoparticles were purchased and citrate stabilized gold nanoparticles have a negatively charged surface which provides a convenient scaffold to attach positively charged proteins (Giljohann et al., 2010). As a result, gold nanoparticles are commonly used for targeted delivery to cells in order to fight cancer and as a diagnostic marker. For instance gold nanoparticles are commonly exploited by conjugating the surface to have an increased affinity for malignant cells (Arvizo, Bhattacharya, & Mukherjee, 2010). Another way gold nanoparticles are utilized to fight cancer is photothermal therapy. Gold NPs that can target cancer cells may act like a thermal scalpel and irradiate heat when exposed to 800-1200 nm of light. Gold nanoparticles that are citrate stabilized and coated with and anti-EGFR (epidermal growth factor receptor) can target HSC3 cancer cells. Other applications are optical communication devices, protein delivery, bimolecular delivery, disease detection, and many other cell-targeting and imaging techniques (Alanazi, Radwan, & Alsarra, 2010). They have been used in immunoassays, protein assays, and capillary electrophoresis. Gold nanoparticles have been known to induce apoptosis in B cell-chronic lymphocytic leukemia (Iravani, 2011).

2.6 Gold Nanorods Production and Applications

Unlike gold nanoparticles, the fabrication of colloidal gold nanorods has emerged only within the last decade (Huang, 2009). The unique shape of gold nanorods caused a

recent upsurge in potential applications within the biomedical industry. Gold nanomaterials have a wide range of applications due to their optical properties. Within the magnetic electrical field of light, the conductive electrons oscillate with a specific resonance known as the surface Plasmon resonance (SPR). The SPR oscillation causes a strong absorption of light and is dependent on particle, size, shape, and structure and dielectric properties of the metal and surrounding medium. Nanorods are considered different because their SPR potential is two directions, unlike spherical gold nanoparticles that only have one. Gold nanorods can have a longitudinal and transverse SPR (Huang, 2009). These different resonances are independent of one another and can be selectively excited(Perez-Juste, 2005). The gold nanorods used in this study were dispersed in water and stabilized with CTAB (cetyltrimethylammonium bromide). CTAB is believed to be a positive surface coating for the nanorods (Gole, 2005) . The general synthesis for gold nanorods with CTAB stabilizer begins with a small gold nanoparticle. The small gold nanoparticle is synthesized by a reduction of a gold salt with a strong reducing agent and capping agent. The reduced metal salts are considered gold seeds and added to another solution with more gold salt, a weak reducing agent and a surfactant directing agent, such as cetyltrimethylammonium bromide (CTAB) (Gole, 2005).

2.7 *Helianthus annuus* (Common Sunflower)

Helianthus annuus (the common sunflower) is a popular annual species that is a food crop as well as an ornamental plant. It is a broad leaf plant with a primary root. According to the USDA, the United States year average market value for the sunflower crop is 446 million dollars (*Crop Values 2013 Summary*, 2014). Sunflower is known to be a

hyper accumulator of metals (Carlson, 1974). In addition, sunflower is known to be a hardy plant that can withstand stress as well as temperatures as low as 25 ° F (4°C)(Berglund, 2011). In addition, according to the United States Department of Agriculture, sunflower is listed as a common plant that can be grown without soil for experimental use (Blankendaal, 1972). As a result, it was chosen as the model plant for this study due to its ability to withstand lower temperatures, its growth capability in the lab and in hydroponics, and it is considered an important crop to the United States.

Chapter 3 Methods

3.1 Sunflower Germination

H. annuus seeds (ProCut Brilliance AN01277) were purchased from Swallowtail Garden Seeds (Santa Rosa, CA). Seeds were germinated according to the procedure by Blankendaal etc. (Blankendaal, 1972). Seeds were placed in a container overnight for approximately 18 hours, and then wrapped in wax paper and DI-soaked paper towels for germination. Paper towels and DI water were all sterilized in a high-pressure sterilizer (TOMY ES-315) at 120°C for 120 minutes. After the DI water and paper towels were sterilized and the seeds were soaked for 18 hours, 6-7 seeds were placed in between the DI-soaked paper towels and loosely rolled in wax paper and placed in a 150 mL beaker with 5 mL of sterilized DI water for 4-6 days in the dark. The seeds were germinated for only 4 days in experiment 1, and for 6 days in experiments 2 and 3.

3.2 *H. annuus* transplantation

For all three experiments, germinated *H.* annuus with roots between 15-30 cm were utilized. Figure 3-1 shows the germinated seedlings after the 6-day germination period and Figure 3-2 is an example of how the germinated seedlings appear after transplantation into the test tubes.

Figure 3-1: Germinated seedlings before transplant

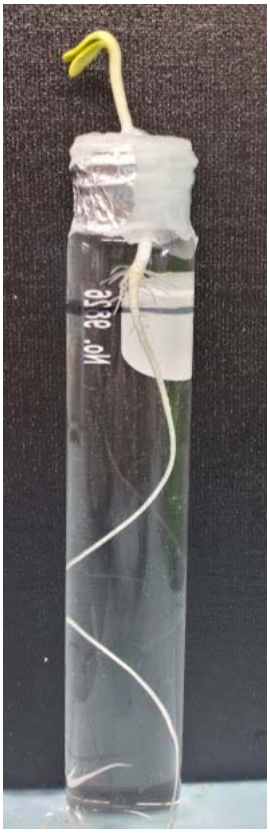

Figure 3-2: Transplanted Seedling

After germination, sunflower seedlings, were placed in 50 mL tin foil wrapped test tubes. Test tubes were filled with 0.10 Hoagland Solution that consisted of: 1 M $Ca(NO_3)_2$, 2 M KNO_3, 2 M $NH_4H_2PO_4$, micronutrients, 20 mM Fe EDTA, 1 M $MgSO^{4-}$, and 1 M NaOH.

Batches for all three experiments were made in 8 L increments. To make an 8 L batch, the following ingredients in Table 3-1 were added to 8 L of water:

Table 3-1: Hoagland Solution Preparatory Method

Ingredients	Amount added to 8 L of DI water(mL)
1 M $Ca(NO_3)_2$	4.8
2 M KNO_3	3.6
2 M $NH_4H_2PO_4$	2.4
micronutrients	2.4
20 mM Fe EDTA	2.4
1 M $MgSO^{4-}$,	1.2
1 M NaOH	Add to pH of 6.8

The amount of NaOH added per batch varied, as it was used to adjust the pH to 6.8. Plants grown in the growth chamber were kept at 25 ± 1°C and photoperiod was operated at 16 hours per day under fluorescent lighting with a light intensity between 120 and 180 µmol m^{-2} s^{1}.

3.3 Gold Nanoparticles

Twenty nm colloidal gold nanoparticles were stabilized with citrate in water by NN labs (Fayetteville, AZ). Figure 3-3 shows a picture of gold nanoparticles in 50 mL containers at a concentration of 0.05 mg/mL as they were received. The absorbance peak for the nanoparticles, according to NN labs, is 520 ± 10 nm in the visible range and the solutions appear dark red. Figure 3-4 shows the 20 nm gold material under Transmission Electron Microscope (TEM) imaging.

Figure 3-3: 50 mL containers of 20 nm Au NPs at 0.05 mg/mL stabilized with citrate and dispersed in H_2O

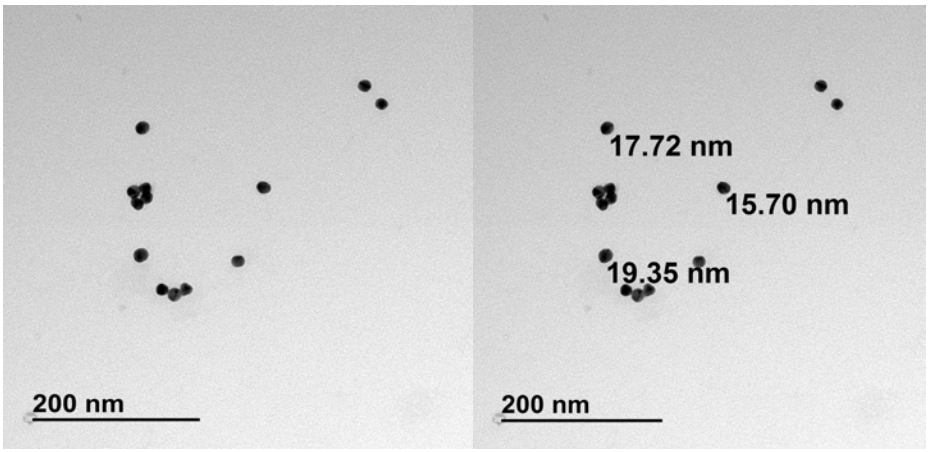

Figure 3-4: Micrograph of 20 nm Gold Nanoparticles in solution under TEM imaging. Picture on the right shows diameter of a few nanoparticles. This picture serves as a reference for the size and electron density of the gold nanoparticles by TEM.

3.4 Gold Nanorods

The gold nanorod solution for Experiment 4 was purchased from Sigma Aldrich Company (www.sigmaaldrich.com) with a maximum absorption wavelength of 650nm and dispersed in H_2O with CTAB (cetyltrimethylammonium bromide) as a stabilizer. Sorption of the CTAB cation on the surface of the gold nanorods imparts a positive charge on the nanorods at pH 6.8. Cetyltrimethylammonium bromide (CTAB) is

used as an antiseptic against bacteria and fungi and is known to be toxic. The gold nanorods were only used in experiment 4. In experiment 4, seedlings were allowed to grow for a week and five sunflower seedlings were exposed to 6.0 mg/L gold nanorods for seven days. The concentration of gold nanorods used is given in Table 3-5 in section 3.8. Figure 3-5 shows images of the gold nanorods under TEM.

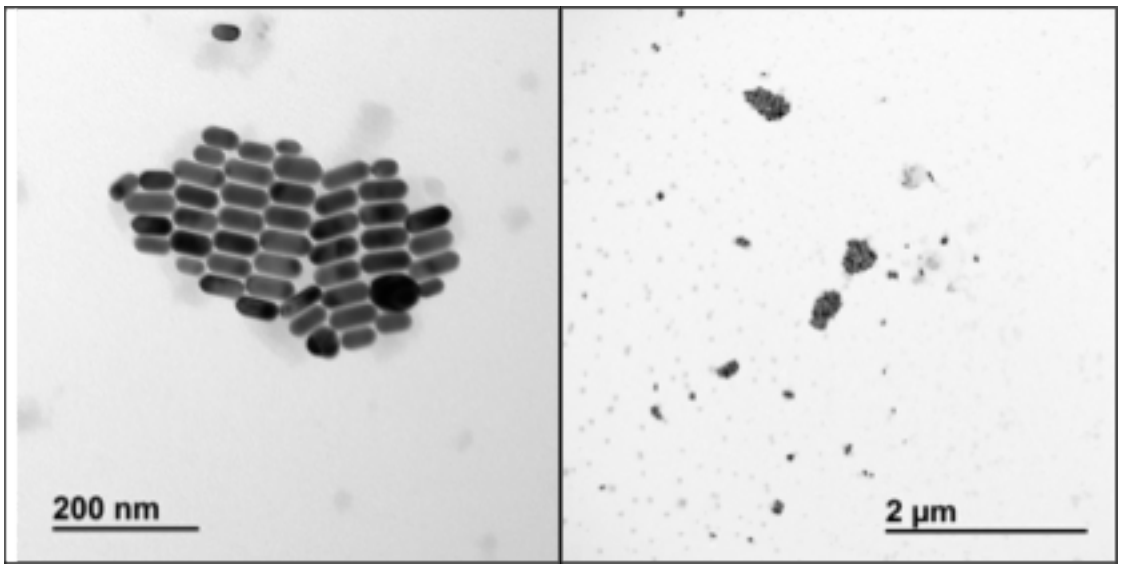

Figure 3-5: TEM images of 25x69 nm Au rods in solution. With permission from (Moradi, 2014).

3.5 Experiment 1-Effect of Temperature

In experiment 1, there were four treatments with 3-4 plants per treatment. Two out of the four treatments were placed in the growth chamber at 25 ± 1°C. The other two treatments were placed in a freezer which operated at an average 7.5°C with a fluorescent light modular strip that was approximately (14 inches) which operated at 16 hours on 8 hours off cycle. The amount of light measured using this single fluorescent bulb was 36.3-36.9 µmol m^{-2} s^{1}. Each non-control treatment was dosed with 3 mL of 20 nm citrate

stabilized gold nanoparticles in water solution that were purchased from NN labs (Fayetteville, AZ). There were also two control treatments that consisted of 4 plants, where there was a control in the freezer as well as a control for the growth chamber. At day 2, root samples of the four treatments were taken for TEM analysis, but were allowed to continue growth. Finally, on day 9, all plants were harvested to measure final wet and dry biomass and samples of the root, shoots, and leaves were taken for TEM analysis. No solution samples remained, for ICP-MS analysis was not performed.

Table 3-2: Nanoparticle Concentrations for Experiment 1

Treatment Temperature	Concentration (mg/L) Control	Concentration (mg/L) NP
Growth chamber (25 ± 1°C)	0.00	3.00
Cooler (7.5°C)	0.00	3.00

3.6 Experiment 2-Uptake and Translocation

In experiment 2, seeds were germinated for six days and all chosen seedlings had a root length between 25-30 cm. The root lengths were recorded during initial transplantation. Stem height was measured during initial transplantation and harvest. There were a total of three treatments: Control, 10.0 mg/L of gold nanoparticles added (A), 14.0 mg/L of gold nanoparticles (B).

Table 3-3: 20 nm citrate-stabilized Gold Nanoparticle Concentration for Experiment 2

Group	Concentration (mg/L)
Control	0.00
A	10 .0
B	14.0

When all seedlings were found to have developed two true leaves, then gold nanoparticles for the specific treatment were added. For experiment 2, the plants were harvested after nine days. Wet total biomass, root, shoot, and leaf mass were recorded. The plants were then placed in the oven for 2 days at 60°C, and final dry total biomass, root, shoot and leaf masses were recorded. During harvest, extra NPs that stuck on the roots were rinsed off into a separate test tube using DI water and saved for analysis. Samples from the original solution and solution washes were centrifuged and stored in freezer for ICP-MS analysis. The dry plant root and leaf matter were lightly mashed using an acetone washed wooden pick to make into smaller sizes for proper ICP-MS preparation. The shoots of the plants were cut into smaller pieces using acetone washed scissors.

3.7 Experiment 3: Concentration Dependency

For experiment 3, the germination procedure was similar to experiment 1 and 2. The seeds were allowed to germinate for six days. Once the seeds germinated, they were transplanted into 50 mL beakers wrapped in tinfoil. Tinfoil was also added to tops of the beaker to attempt to exclude light and to accurately mimic light conditions in the subsurface. Before transplanting, root length and biomass were recorded, as well as stem height at the time of transplanting. Once the plants developed two true leaves, they were dosed with three different concentrations shown in Table 3-4.

Table 3-4: Nanoparticle concentrations for Experiment 3.

Group	Concentration (mg/L)
Control	0.0
A	4.0
B	10.0
C	40.0

Table 3-4 shows the concentrations the four treatments were inoculated with. At the time of inoculation, 1.0 mL solution samples were taken at day zero, two, five, and eight. After harvest, plants were weighed for wet biomass and placed in a drying oven for two days at 60°C , and then weighed for dry biomass. In addition, during harvest, nine samples were set aside in order to make a comparison between roots unwashed and roots washed. For three samples of each treatment, a sample of the root was cut off and not rinsed with water.

3.8 Experiment 4: Nanorods versus Nanoparticles Toxicity to Sunflower

For this extra experiment, 5 plants that were germinated for experiment 3 were exposed with 6.0 mg/L of gold nanorods. The plants were allowed to grow for seven days and then were exposed to gold nanorods for seven days. The concentration of gold nanorods used for this experiment is shown in Table 3-5:

Table 3-5: Gold Nanorod concentration and size used in Experiment 4.

Gold Nanorods	Stabilized in	Size	Concentration
	CTAB (Cetyl trimethylammonium bromide)	25x69 nm	6.0 mg/L

Table 3-5 shows the gold nanorods concentration used (6.0 mg/L) as well as the chemical that was used to stabilize the nanomaterials. After seven days, photos were taken of the gold nanorod solution and the appearance of the roots verse control. Final biomass and stem height were measured and compared to the biomass and stem height of sunflower seedlings in experiment three.

3.9 Experiment 5-Sorption Isotherm of AuNPs to root

The methodology for this experiment is based on procedural methods from Burken and Schnoor 1998 (Burken & Schnoor, 1998) This experiment was performed using 15 plants that were germinated during experiment 3. The sunflowers were grown in test tubes for eight days. Sunflowers were removed from the test tubes and the roots were cut from the aboveground biomass. The roots were weighed and placed into a new test tube in one of the four treatment categories (Table 3-6).

Table 3-6: Experiment 4 Concentrations

Treatment	Concentration (mg/L)
Control	0
1	2.0 mg/L
2	5.0mg/L
3	10.0 mg/L
4	15.0 mg/L

Table 3-6 shows the concentrations used in the experiment. The solutions from all 15 samples were measured using ICP-MS and the roots were also measured for ICP-MS. From the ICP-MS results, a Kd value was estimated.

3.10 TEM Analyses

For TEM analyses, plant tissue samples from roots, shoots and stems were collected and analyzed for all three experiments. TEM analyses were conducted on roots for experiment 1 using Spurrs reagent with osmium technique. For experiment 2, two different TEM preparatory methods were used to determine which method could potentially provide better images) of roots, shoots and leaf samples (Spurrs with osmium vs. Lemon Resin White).

3.10.1 Spurrs with Osmium TEM preparation

Samples of leaf, shoots and roots were separated and cut into small (approximately 1 mm^3) size using a razor and transferred to ½ strength Karnovsky's

fixative (Karnovsky, 1965). The samples were stored at 4°C until ready to prepare for TEM. After initial fixation took place using ½ strength Karnovsky's fixative, several buffer washes of 0.1 M cacodylate solution removed the excess fixative. The samples were then post-fixed for 90 minutes in 1% osmium tetroxide in 0.1 M cacodylate buffer containing 1.5% potassium ferrocyanide (Kato, 1967). Several changes of wash buffer and one of distilled water followed. Samples incubated for 1 hour with an en-bloc stain of 2.5% uranyl acetate (Terzakis, 1968) at this point followed by a very slow dehydration in increasing concentrations of acetone starting at 15% acetone. When the samples had been in at least 3 changes of 100% acetone, a 1:1 solution of acetone and propylene oxide was applied for 30 minutes. Two incubations of 1 hour in 100% propylene oxide prepared the tissues for a mixture of propylene oxide and Spurrs epoxy resin. A gradual infiltration of the resin occurred by small incremental increases of Spurrs resin (Spurr, 1969; Spurr & Harris, 1968) until a 100% Spurrs solution was reached. To insure complete infiltration, samples were placed in three successive changes of Spurrs resin over a six-hour period. Finally the plant tissue samples were placed into flat silicon embedding molds and cured at 70°C for 48 hours. The resulting blocks were cut at 80nm using a Leica EM UC6 Ultra microtome (Solms, Germany) and placed on (Electron Microscopy Sciences, Hatfield, Pennsylvania #15820)-coated grids. The samples were imaged using a JEOL JEM-1230 transmission electron microscope (JEOL USA, Inc.)

3.10.2 Lemon Resin White (no osmium) for TEM

TEM samples were prepared using the lemon resin white technique rather than Spurrs, based on research provided by Carpentier etc. (Carpentier, Abreu, Trichet, &

Satiat-Jeunemaitre, 2012). For this procedure, the samples were stored in the ½ strength Karnovsky's fixative. Next, there were multiple buffer washes using 0.1 M cacodylate solution to remove the excess fixative. Next a series of ethanol dilutions were used at 15 minute intervals to 95% EtOH. The samples were in 95% EtOH for 30 minutes and two 100% EtOH runs were completed in 30 minutes intervals in order to guarantee plant tissue dehydration. Then, the LR white was introduced to samples in a 1:1 ratio with 100% EtOH. Next 100% LR white was used for two runs at 1 hour each to wash out remaining EtOH. Finally the samples were cured for 3 hours under UV light on ice. The resulting blocks were cut at 80nm using a Leica EM UC6 Ultra microtome (Solms, Germany) and placed on formvar (Electron Microscopy Sciences, Hatfield, Pennsylvania #15820) -coated grids. The samples were imaged using a JEOL JEM-1230 transmission electron microscope (JEOL USA, Inc.).

3.11 ICP-MS procedure

3.11.1 ICP-MS procedure for solutions

The gold concentrations in solution samples and leaf, roots, and stem samples were analyzed by ICP-MS (Thermo X-series II, USA) following the general methodology of Pitcairn et al. (Pitcairn, Warwick, Milton, & Teagle, 2006). First, Teflon vials (Savillex™) were pre-treated with 10x diluted aqua regia, 2% HNO_3 and 2% HCl for two hours to remove any excess gold that might exist in the containers. Then the vials were rinsed with HNO_3 and DI water and allowed to dry overnight. For filtered and non-filtered solution samples, 1 mL of solution sample was exposed to gold nanoparticles or 1.0 mL of filtered solution samples were aliquoted into vials. The filtered samples were filtered using

Amicon Ultra-4 3K (Merck Millipore Ltd.) centrifugal filter devices. The solution samples were filtered in order to determine if the gold in the solution samples were Au^{3+} or AuNP. After the liquid from the samples were allowed to evaporate for 3 hours at 90 °C on the hot plate, 3 mL of aqua regia was used to digest the samples for 6 hours at 90 °C. The samples were dried again at 90 °C on the hot plate until all the liquid evaporated. Internal standard Re solution 41.7 µL (1.64 µg/mL) was added to the vials as well as 4 mL of 2% HNO3 and 2% HCl solution in order to dissolve the remaining gold and measured in ICP-MS.

3.11.2 ICP-MS Procedure for Tissue

Oven dried leaf and root samples were grounded up using a flat edged stick for the roots and leaves. The stems were chopped into smaller pieces using a sterilized blade. Leaf, shoot, and root samples were weighed and placed in Teflon vials (Savillex™) and digested overnight at 80 °C in a mixture of 1 mL of hydrogen peroxide and 3 mL of nitric acid. Then, 4 mL of hydrochloric acid was added and the samples were heated for an additional 4 h. Digested tissue samples were quantitatively transferred and diluted into 30 mL bottles using 2%HNO3-2%HCl, after addition of 0.25 mL of Re solution (1.64 µg/mL) as an internal standard. All tissue samples were filtered with a 0.2 µm sterile syringe filters (Millipore™) prior to analysis by ICP-MS.

Chapter 4 Results

4.1 Experiment 1-Effects of Temperature.

One hypothesis of gold nanoparticle uptake into the cytosol of plant cells was via endocytosis (the entry of particles or fluids into cells by methods other than diffusion or carrier proteins). It is known that endocytosis is inhibited under cold temperatures, which was to be tested in Experiment 1(Liu, 2009).

4.1.1 Appearance

Figure 4-1: Appearance of plants during Experiment 1. Image on left shows two seedling treatments, the control and seedlings exposed to 3.0 mg/L of NP, in the growth chamber. On the right are two seedlings exposed to 3.0 mg/L of gold nanoparticles after 9 days in the cooler and growth chamber respectively.

Figure 4-1 shows two photographs for plants after an exposure period of nine days to an initial concentration of 3.0 mg/L gold NPs (20 nm). The figure on the left shows a control (no nanoparticles) and the results of 3.0 mg/L NP initial concentration exposure after nine days. It appears that the 3.0 mg/L treatment contained more biomass compared to the control. The figure on the right shows two seedlings exposed to an initial concentration of 3.0 mg/L of gold nanoparticles at 7.5°C and 25°C respectively for nine

days. The colder temperature appears to have a significant negative effect on the total biomass-growth which was slower at 7.5°C.

4.1.2 Biomass

For Experiment 1, 3.0 mg/L AuNP (20 nm) concentrations was chosen as a starting concentration to test the relationship between *H. annuus* seedlings and gold nanoparticles

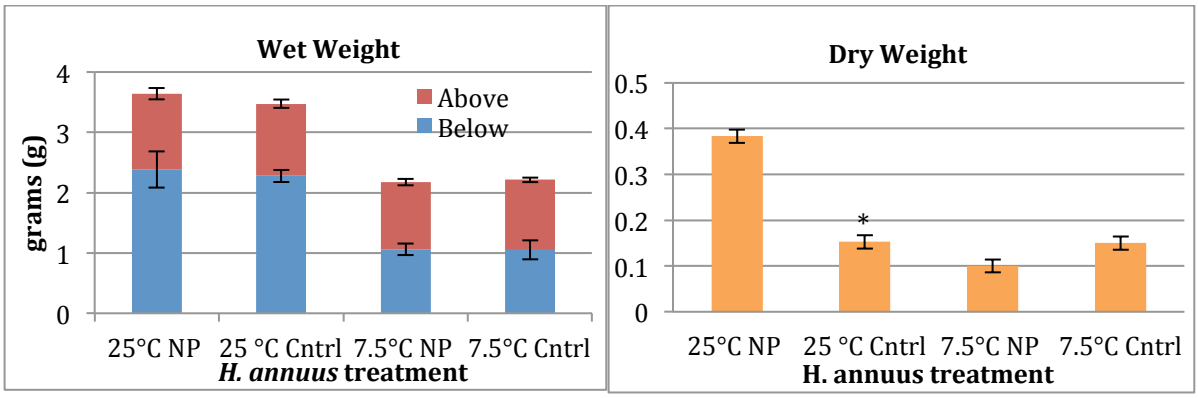

Figure 4-2: Wet biomass (left panel) and Dry biomass (right panel) exposed to 3.0 mg/L of 20 nm gold NP at two different temperatures for nine days. For the control n=4 and for the NP treatment n=3.

Figure 4-2 shows the overall wet and dry biomass for Experiment 1 at the end of nine days. Looking at the left panel, side of Figure 4-2, the overall wet biomass for Experiment 1 shows no statistical significance between treatments within the same temperature. Statistical significance was defined as a p-value less than or equal to 0.05. In general, there were no significant differences between the controls and the treatments at either (7.5° or 25°C). However, it was clear that there was greater growth of biomass during the experiment at 25°C than at 7.5°C which was expected. In the panel on the right, one anomaly is evident. There was a significant difference between the control and the treatment at 25°C (p-value 0.02). This was likely the result of an artifact (experimental error) due to the oven drying process.

4.1.3 Transpiration

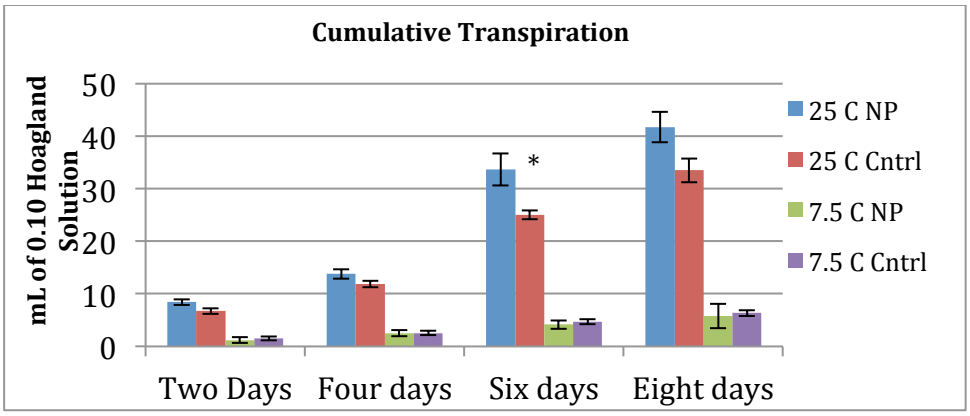

Figure 4-3: Cumulative transpiration for Experiment 1.

Figure 4-3 shows cumulative transpiration over the course of eight days. As expected, the colder temperature experiment yielded less transpiration for both the controls and the NP exposure. Growth was small at 7.5°C in both cases, but the sunflowers continued to transpire and grow, despite the cold stress. There was a statistically significant difference in transpiration between nanoparticles and control on day six at 25°C with a p-value of 0.018. However, the same statistical significance did not occur on day eight (p-value 0.118). Overall, the results in figure 4-2 and 4-3 did not show evidence of phytostimulation (greater growth and transpiration) for 3.0 mg/L of gold nanoparticles. There also was no evidence of phytotoxicity (less growth and transpiration).

4.1.4 TEM Imaging

The next goal was to determine if cold temperature (7.5°C) could completely prohibit AuNP uptake, suggesting that uptake could be via endocytosis. In order to examine this, root samples were taken for TEM imaging at the two-day mark. TEM

samples were also taken at the ten-day mark for roots, shoots and leaves for all treatments. If there was a different in uptake, it should have appeared early in the experiment.

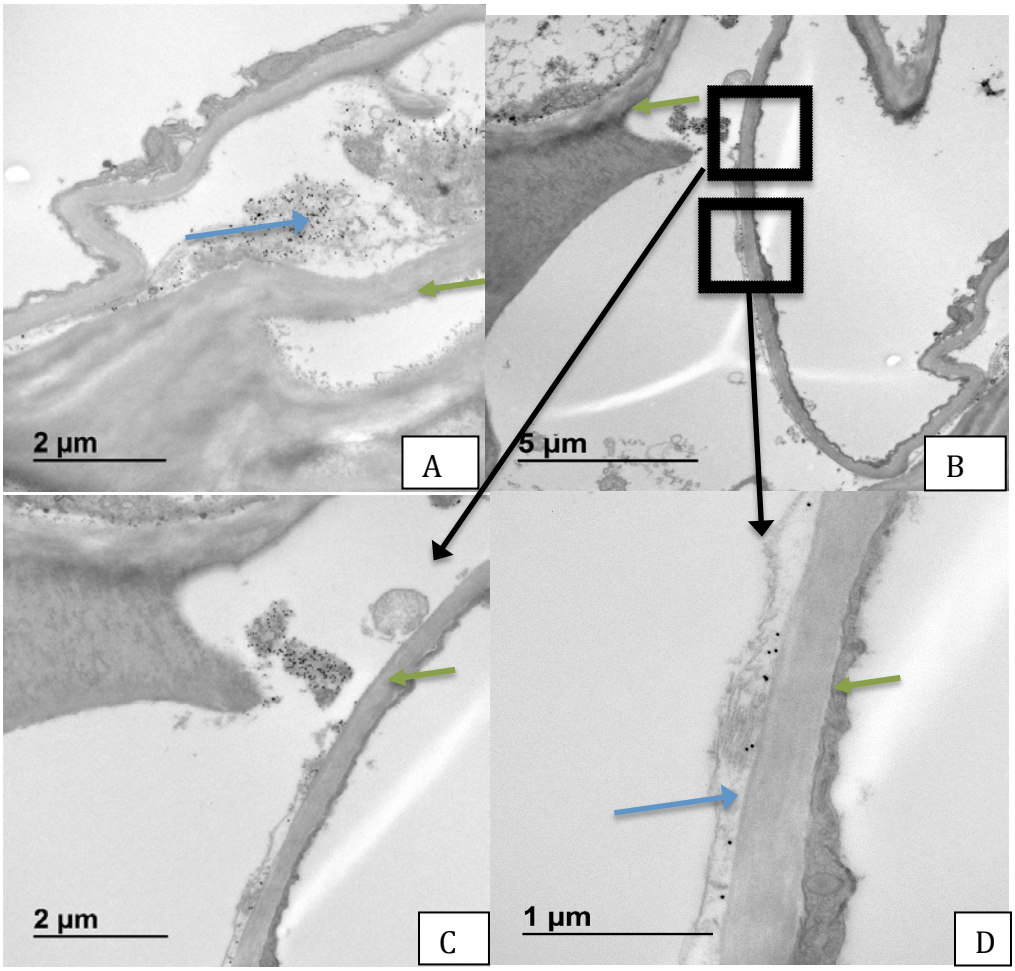

Figure 4-4: TEM Images of 2 day root samples at 7.5°C when exposed to 3 mg/L of Au NPs 20 nm. Magnification: A 30K, B 3K, C 3K, and D is 8K. Blue arrow-NPs. Green arrow-Cell wall.

Figure 4-4 shows TEM images of roots samples after two day exposure to NPs at 7.5°C. In photo A at a magnification of 30,000X, the NPs appear to be in the cytoplasm, just inside the cell membrane. In B at a different location in the root and at a magnification of 3,000X, the NPs also appear to be in the cytoplasm. Photo D is a magnification of B, and it is clear that the NPs are right in between the cell wall and cell membrane. Photo C is at a

magnification of 3,000X and shows NPs in the cytoplasm, further away from the cell membrane. Overall, Figure 4-4 indicates that despite the lower temperature, 20 nm AuNPs do appear to get inside the plant cell and can be found in the cytoplasm or at the cell wall. Since research suggests endocytosis is inhibited at 4°C, and this experiment was performed at 7.5°C, due to problems with the cooler, the endocytosis mechanism theory cannot be completely ruled out. However, it appears that endocytosis may not be the predominant mechanism for the entry of NPs into the cytosol based on the lack of difference between uptake of nanoparticles at 25 and 7.5°C.

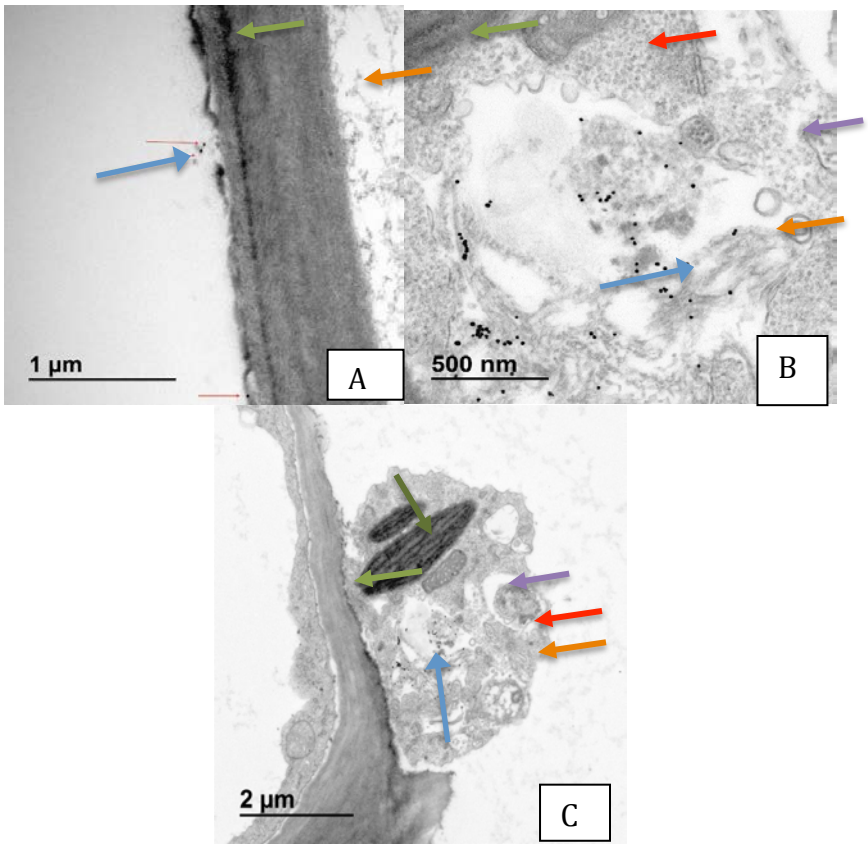

Figure 4-5: TEM images of roots exposed to 20 nm of 3 mg/L Au NPs after 2 days at 25° C .Magnification: A-8K B-12K C-3K. Green cell wall, Blue- NPs, Orange-cytoplasm, Red- nuclear envelope Purple- transport vesicles, Dark green- chloroplast.

Figure 4-5 shows TEM images of roots after 2 day exposure to 3.0 mg/L of Au NPs at 25°C. Photo A, with a magnification of 8 ,000X shows NPs outside the cell wall. Photo B shows them on the inside of the cell wall in the cytoplasm, surrounded by different transport vesicles and on the far right there appears to be a part of the nuclear envelope. Photo C shows a chloroplast, a mitochondrion and transport vesicles. It was surprising to see a chloroplast in a root cell, however, this is possibly due to the fact that Parafilm covered the top of the test tube in experiment 1 and some light reached the roots. For

subsequent experiments, aluminum foil was carefully wrapped around all test tubes including on top of the Parafilm.

4.1.5 Summary of Experiment 1

The results from experiment 1 showed no stimulatory or inhibitory effect of 3.0 mg/L AuNPs on sunflower seedlings. Also, despite the temperature, NPs were found within the root cells and after two days. According to the literature review, endocytosis is inhibited at 4°C. However, at the coldest temperature studied in this work, 7.5°C, it was clear that 20 nm Au NPs were found in roots after two day exposure. The results indicate that the reaction between NPs and the root system was fast and was not inhibited at 7.5°C, therefore endocytosis was apparently not the predominant mechanism. In addition, *H. annuus* seedlings at the lower temperature had a reduction in biomass. However, this could be a result of the lower light intensity compared to the growth chamber as well as temperature. From this experiment at 7.5°C, it is not possible to prove or disprove the hypothesis of endocytosis as a mechanism for nanoparticle uptake by plant cells, but it is clear that nanoparticles were taken up by seedlings still growing at this relatively cold temperature.

4.2 Experiment 2: Uptake and Translocation

4.2.1 Appearance:

Figure 4-6: After nine-day exposure to 20 nm Au NPs, photos before harvest. Both photos show plants in following order: 0 .0mg/L, 10.0 mg/L and 14.0 mg/L.

Figure 4-6 includes two photos of after nine days, after nine days of nanoparticle exposure to sunflower seedlings; each showing a control, 10.0 mg/L initial concentration exposure of AuNPs, and a 14.0 mg/L initial concentration exposure. As shown by Figure 4-6, there were no differences among plant appearances. All three seedlings on the left and right had the same height and number of leaves and looked bright and green. The only visible differences were the color of the hydroponic solutions and roots. In the figure on the right, the middle and the far rights seedlings clearly showed the presence of NPs accumulating on the roots.

4.2.2 Biomass

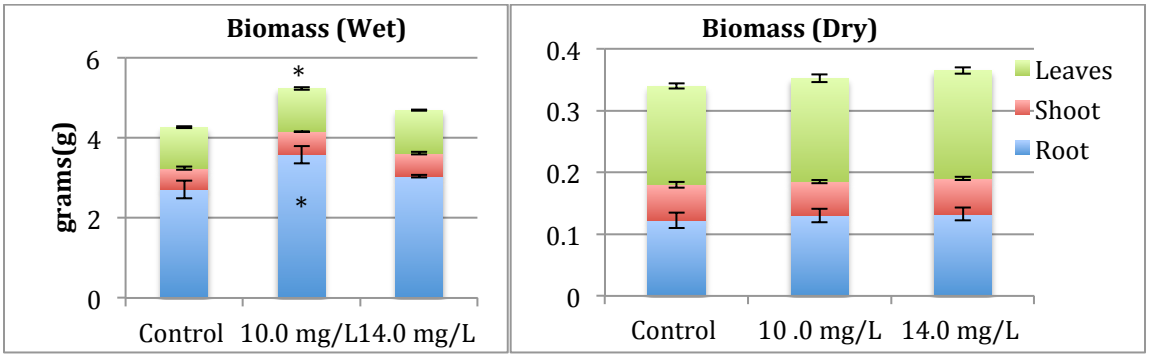

Figure 4-7: Biomass of sunflowers. On the left (wet) and right (dry) for plants exposed to 20 nm Au NPs for nine days.

Figure 4-7 shows the wet and dry biomass for plants at the time of harvest for Experiment 2, for the control, 10.0 mg/L treatment, and 14.0 mg/L treatment (n=4.). Dry biomass measurements corroborated the wet biomass data, showing the same general pattern. For wet biomass, roots at the 10.0 mg/L concentration were significantly greater than the roots biomass for the control with a p-value of 0.03. In addition, when comparing the whole plant (root, shoots, and leaves), the p-value between control and 10.0 mg/L of Au nanoparticles was statistically significant with a p-value of 0.018. However, the dry biomass did not indicate the same significance. Dry biomass showed that there was no statistically significant difference between any of the three treatments. The wet biomass treatments at 10.0 mg/L could be an anomaly, but the overall increase in biomass was not significant at 14.0 mg/L exposure concentration. Considered together, the results show that exposure to 10.0 mg/L and 14.0 mg/L nanoparticle concentrations did not stimulate nor impede growth of biomass (no toxicity or phytostimulation).

4.2.3 Biomass change over time

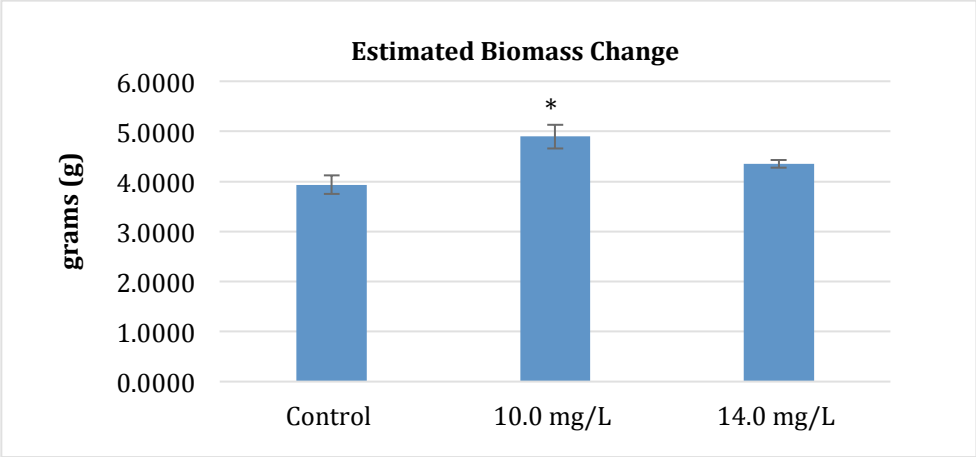

Figure 4-8: Wet Biomass changes from transplant to harvest (14 days) for three different exposure concentrations to 20 nm AuNPs. For all three concentrations n=4.

Figure 4-8 shows the estimated wet biomass change over time (initial biomass was not taken for Experiment 2). An average initial biomass was found based in experiment 3 and applied here to measure an estimated biomass change. This is an accurate estimation because all the seedlings were chosen based on the same general appearance and root length between 25-30 cm. As a result, at the time of transplantation for Experiment 2, the weights were approximately equivalent. It is reasonable to assume that at the time of transplantation all germinated seedlings were approximately 0.3-0.4 grams. Comparing the 10.0 mg/L treatment to the control, the biomass indicated a significant difference with a p-value of 0.018. Comparing the 10.0 mg/L to 14.0 mg/L treatment, there was no statistical significance (0.07). Comparing the biomass change (Figure 4-8) to biomass (Figure 4-7), the bar of each treatment gave approximately the same value, indicating at the time of transplant, the seedling weights were small and insignificant.

4.2.4 Transpiration

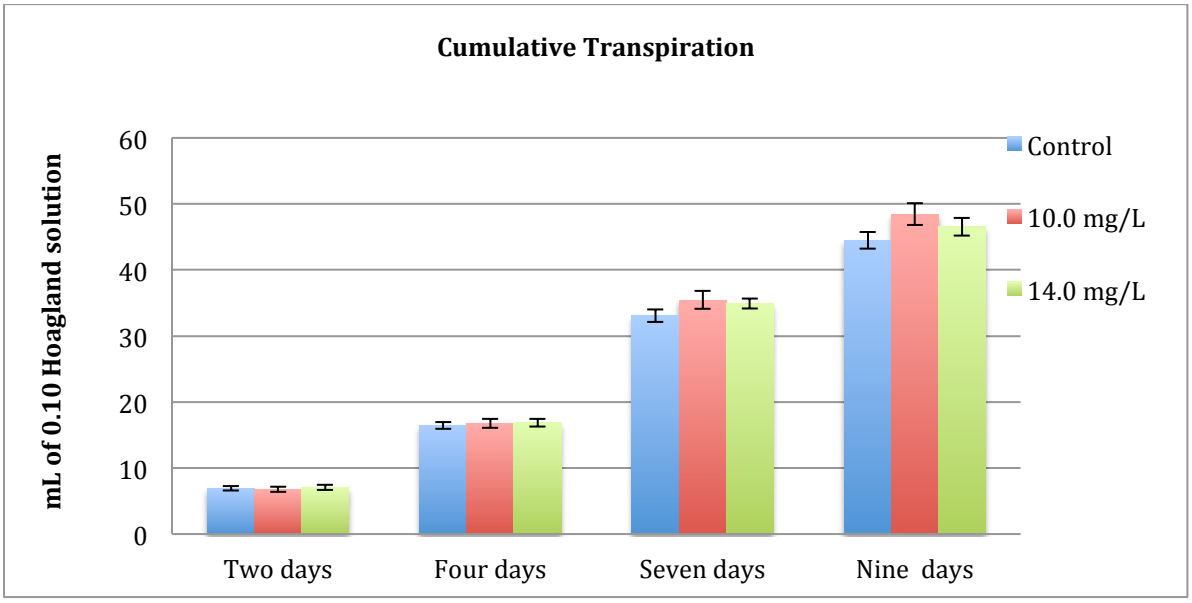

Figure 4-9:Cumulative Transpiration for Experiment 2, exposure of 20 nm AuNPs for nine days.

Figure 4-9 shows cumulative transpiration of three concentrations over time. Overall, it indicated that all three treatments were undergoing transpiration continuously during the experiment. On day nine, it appears that both nanoparticle-dosed treatments transpired slightly more than the control plants. According to Figure 4-9, the 10.0 mg/L treatment was greater than the control. However, for day seven and day nine this was not significant with a p-value of 0.14 and 0.06, respectively. Once again there was no strong evidence that gold NP exposure either inhibited or stimulated sunflower seedling growth. There was a significant difference in overall growth for the 10.0 mg/L treatment after nine days, but this was likely a random variation.

4.2.5 ICP-MS Solutions

For ICP-MS on the solutions, during harvest, the roots were rinsed and the DI rinse solutions were put into another test tube. This provides information on [Au] that rinsed off (lightly sorbed to the roots) compared to the nanoparticles that were strongly sorbed to the plant

root or taken up inside the root tissue. ICP-MS samples were collected during harvest (day 9). In addition to rinsed and not-rinsed root solution samples (whole water samples), the rinsed and not-rinsed root solution samples were filtered (filtered samples) in order to operationally determine "dissolved" gold ions [Au(III)] in solution. If there were detectable amounts in filtered samples, this would be indicative that Au(III) was in solution and not AuNP. Of course, it is possible that some very small diameter NPs are able to bypass the filter.

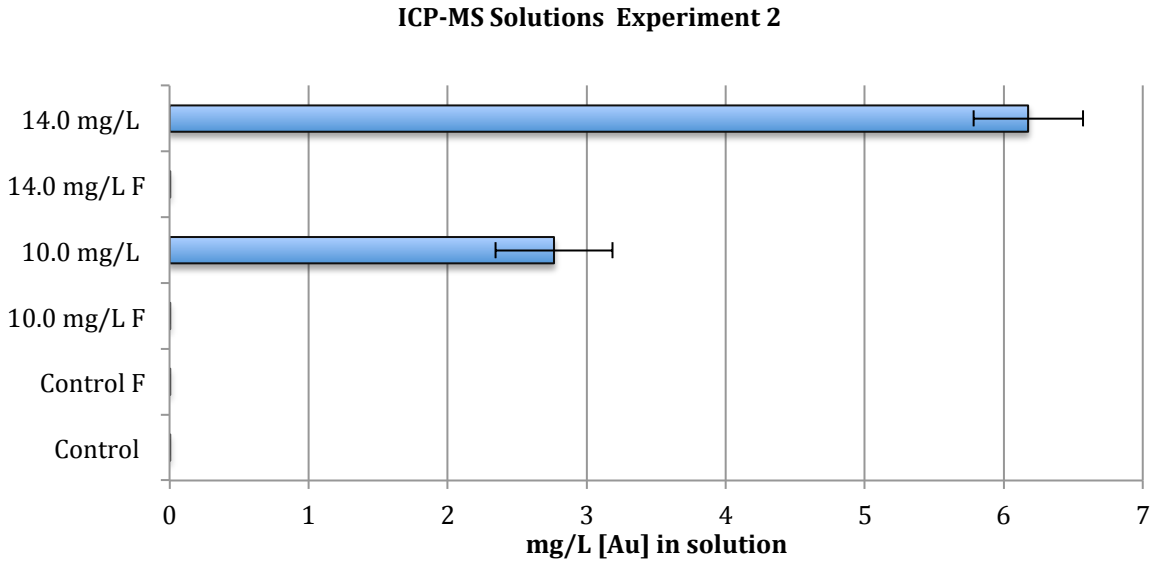

Figure 4-10: ICP-MS of Experiment 2 solutions (filtered vs. unfiltered) to determine potential dissolution and estimated amount that sorbed. (F-filtered)

Figure 4-10 shows the results of gold concentration of control, unfiltered and filtered solutions. The results of filtered and control samples were near zero. These results verify that [Au] in solution were as NPs and not dissolved ions such as Au (III). Filtration always removed the nanoparticles to below detection in all cases.

QA/QC. The filtered samples were replicated, and both times showed the gold in solution for all filtered samples as below detectable limits. ICP-MS analyses for the solutions in Experiment 2 were repeated three times because the ICP-MS machine has a memory while

conducting its measurements. Au is a very "sticky" metal in ICP-MS instrumentation and it was unclear what would be the best order to measure the samples. When conducting ICP-MS on gold it is imperative to analyze the samples in order from lowest suspected [Au] to highest or else samples might contain bias from high concentrations. Therefore, analyses were performed, three times and averaged in order to get a more accurate measurement. The results for the concentration of [Au] in DI rinse solution and final solution can be found in Figure 4-12.

QA/QC. Each time the ICP-MS is used, it must be calibrated to the element and dilutions must be corrected for. Figure 4-11 shows the calibration curve results for all individual ICP-MS trials of Experiment 2 solutions.

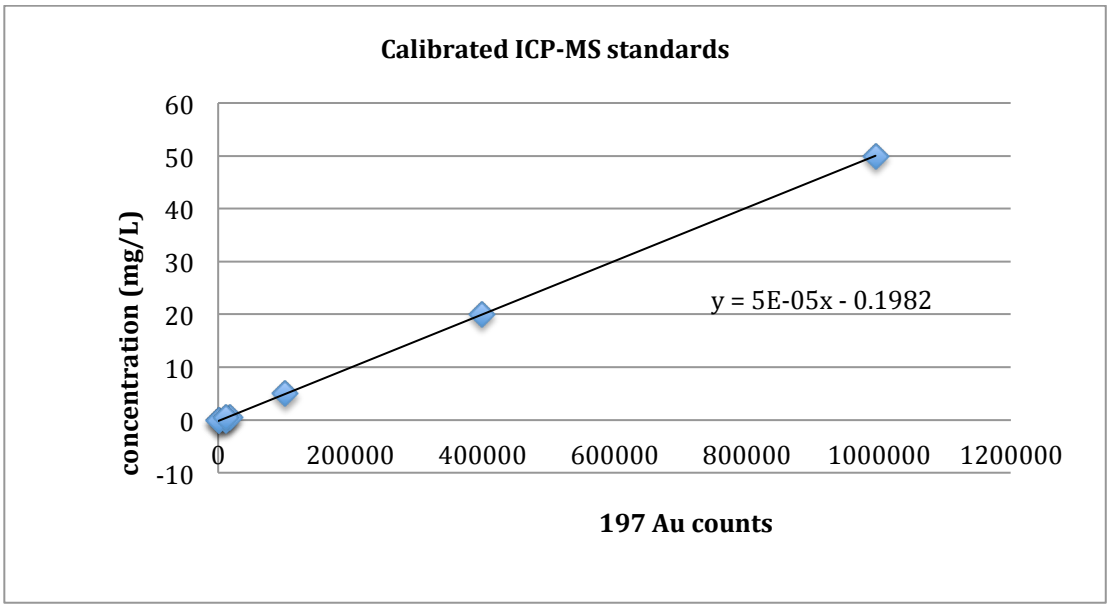

Figure 4-11: Calibration Curve for all experiment 2 solutions.

The QA/QC results for four different days of analyses show that the ICP-MS instrument provided very linear calibration curves for concentration of nanoparticles vs. counts detected. The QA/QC shows that the calibration was very consistent over time and that our solutions used to create the calibration curve did not change over time for all ICP-MS trials. (Appendix Table A-

1) Next, a comparison between average DI rinse water concentrations and final solutions for Experiment 2 can be seen are shown below (Figure 4-12).

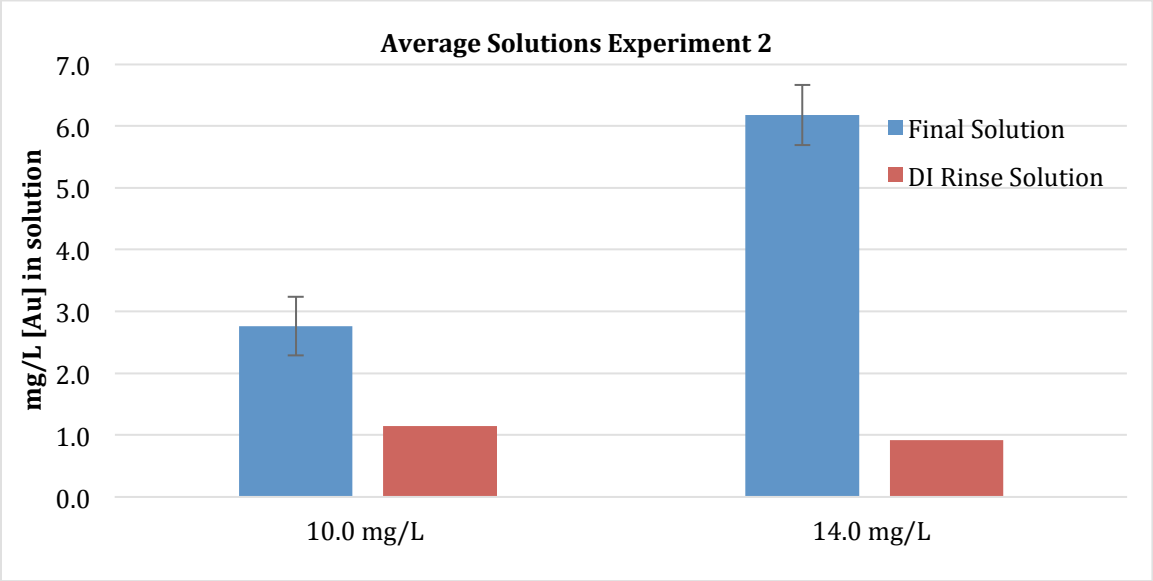

Figure 4-12: Roots were rinsed in separate test tubes with DI water (DI Rinse Solution) compared to the original solution roots were in (Final Solution).

Figure 4-12 shows the difference between the [Au] in solutions vs. the loosely sorbed [Au] that was easily rinsed off with DI water. These are the average results from the trials. It appears that approximately 1.0 mg/L of [Au] was loosely sorbed to the 10.0 mg/L treatment roots. For the 14.0 mg/L, it appears that even less [Au] was loosely sorbed. This indicates that those percentages of AuNPs were sorbed loosely to the outside of the roots and the remainder of the AuNPs were uptaken inside the root tissue as confirmed by TEM images. The final [Au] in solution was found by taking the initial concentration of [Au] in the 10.0 mg/L or 14.0 mg/L treatment and subtracting by the final [Au] solutions. Those results are shown in Figure 4-13. Results indicated that sorption to roots was extensive and 6-7 mg/L were sorbed/uptaken by roots between the beginning of the experiment and the end (9 days).

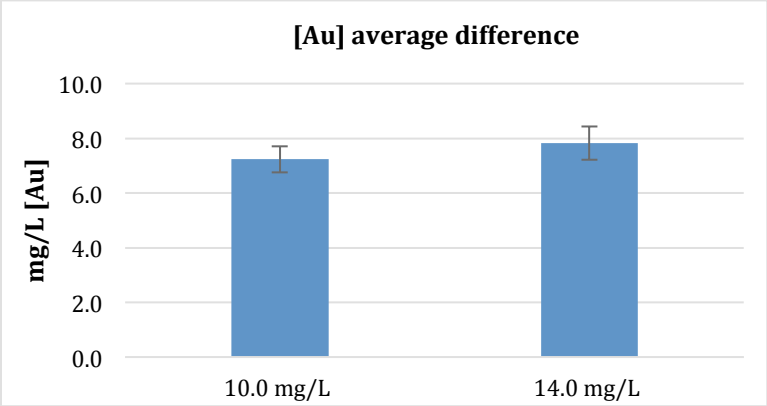

Figure 4-13: Change in solution concentration from initial exposure dose (10.0 mg/L or 14.0 mg/L) to harvest at the end of the experiment (t=9 days).

Figure 4-13 shows the change in solution concentration of Au over the duration of the experiment. Although time zero samples were not collected for experiment 2, during the nine days, both treatment solutions had an overall change in NP concentration between 7-8 mg/L. There was no significant difference in [Au] concentration change between 10.0 mg/L and 14.0 mg/L with a p-value of 0.5.

Overall the ICP-MS solutions of Experiment 2 (Figure 4-10 and Figure 4-12) indicate that there was no chemical reduction and dissolution of AuNPs into Au (III) species in the treatments, and no gold was detected in control samples.

4.2.6 ICP-MS Tissue

ICP-MS analyses were performed on the solutions, roots, stems and leaves. This investigator was concerned that the counts in ICP-MS would be so low in the plant tissue that none would be detectable (potentially a sensitivity problem at extremely low concentrations). Therefore 0.45 ppm Au was added to the leaf and tissue samples for Experiment 2. When roots were analyzed, however, no Au was added because it was recognized that concentrations/counts

for the roots would be larger and detectable. The stem and leaf samples were run twice (replicates) on the ICP-MS instrument as a matter of QA/QC. The results of the two runs were averaged and are shown in the figures below. The individual results from both runs are in the appendix. ICP-MS results of the roots, stems and leaves are shown in the following figures: Figure 4-14, 4-15 and 4-16.

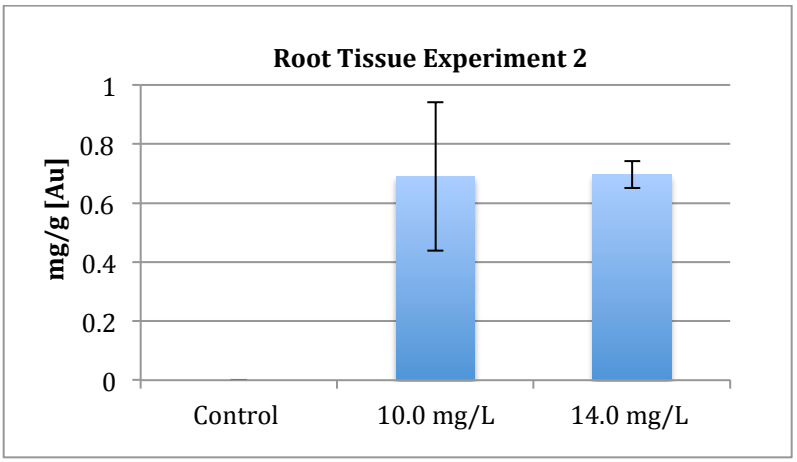

Figure 4-14: ICP-MS [Au] in mg/g of root tissue exposed to 20 nm AuNPs for nine days (n=4).

The ICP-MS results can be seen in Figure 4-14. Results showed that NPs sorbed to the roots. There was no statistically significant difference between the root treatments of 10.0 mg/L and 14.0 mg/L. This makes sense because there was not a large difference in the [Au] solutions between the two treatments and there was variability among replicates. TEM images showed evidence of AuNPs in root tissues (Section 4.2.7).

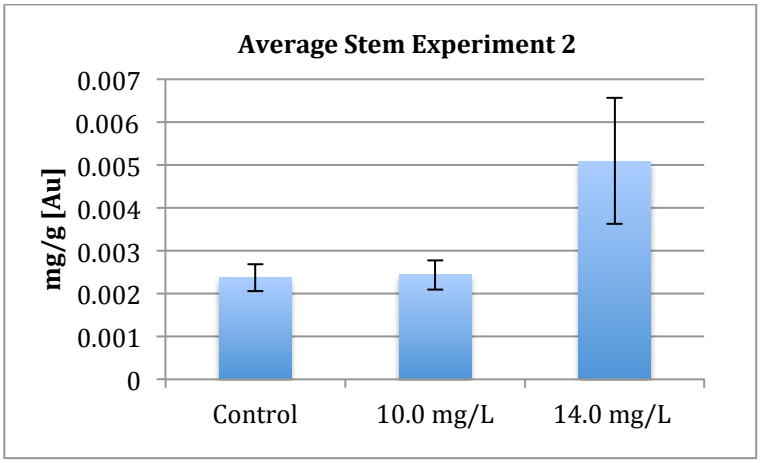

Figure 4-15: [Au] concentration in stems after nine-day exposure to 20 nm AuNPs. Control (n=3), 10.0 mg/L (n=4), 14.0 mg/L (n=4).

Gold was added to all three treatments for the stem and the leaves (0.0 mg/L , 10.0 mg/L and 14.0 mg/L) because concentration were expected to be so low that a "spiked addition" was thought necessary for gold counts to register on the ICP-MS. ICP-MS analyses were run on each triplicate two times. Comparing the 10.0-mg/L treatment to the control treatment, no statistical difference was detected (p-value 0.9). There was no significant difference between 14.0 mg/L compared to the control either (p-value 0.19). This shows no statistical evidence of translocation from the roots to the shoots and also nanoparticles were not evident in corresponding TEM images (See Appendix Figure A-5).

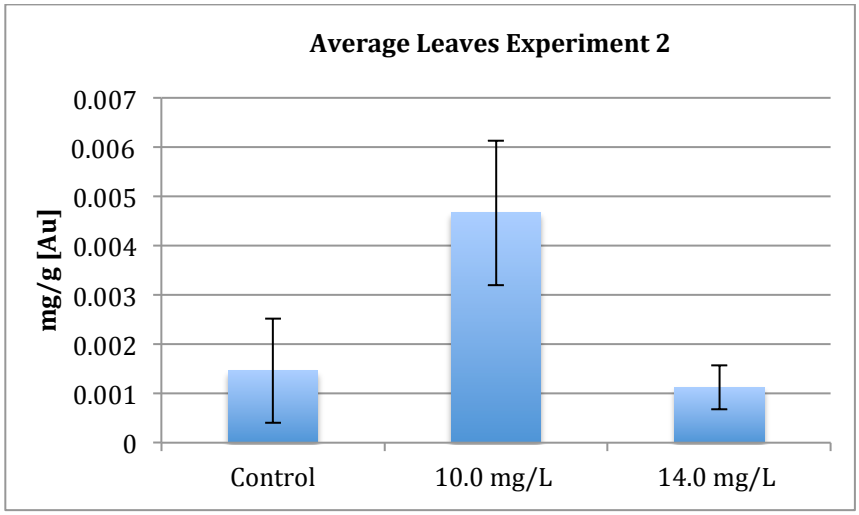

Figure 4-16: [Au] in leaf tissue that were exposed to 20 nm AuNPs for nine days. (n=3) for control, 10.0 mg/L and 14.0 mg/L

Figure 4-16 represents the amount of gold in the leaf tissue. Gold was added to control tissues and to both treatments as before (0.45 ppm Au). There was no statistical difference between the 10.0 mg/L treatment and the control (p-value 0.17). Also, there was no statistical difference between 14.0 mg/L and the control with a p-value of 0.76. Overall, looking at the concentrations (mg/g of Au) within the stem and leaves (Figure 4-15 and 4-16) the values are in the thousandths of mg/g. Since the values are so small and there was no statistical difference between the control and the treatments, it can be concluded that NPs do not translocate significantly between the roots and leaves of sunflower seedlings. This was corroborated by TEM observations in which nanoparticles were not visible in TEM images of the stems and leaves of sunflowers. Unlike the stems and leaves, gold was detected and sorbed to the roots, both inside the root tissue and on the outside (which could be rinsed off). However for the leaves and shoots, TEM images did not show the presence of Au nanoparticles, indicate a lack of translocation of nanoparticles.

4.2.7 TEM Imaging

Figure 4-17 shows the TEM images for root samples, which clearly indicate the presence of nanoparticles. The modified method without osmium was conducted because previous TEM images for experiment 2 did not show the presence of NPs definitively (See photos in Appendix). Kathy Walters, Central Microscopy Laboratory, suggested that this was because osmium is hydrophobic and caused parts of the cell (such as the cell membrane) to appear dark. AuNPs are easy to spot on TEM images because gold is electron dense and appears dark. The clearest TEM images were observed in root samples in the 10.0 mg/L treatment, which corroborated with ICP-MS solution data.

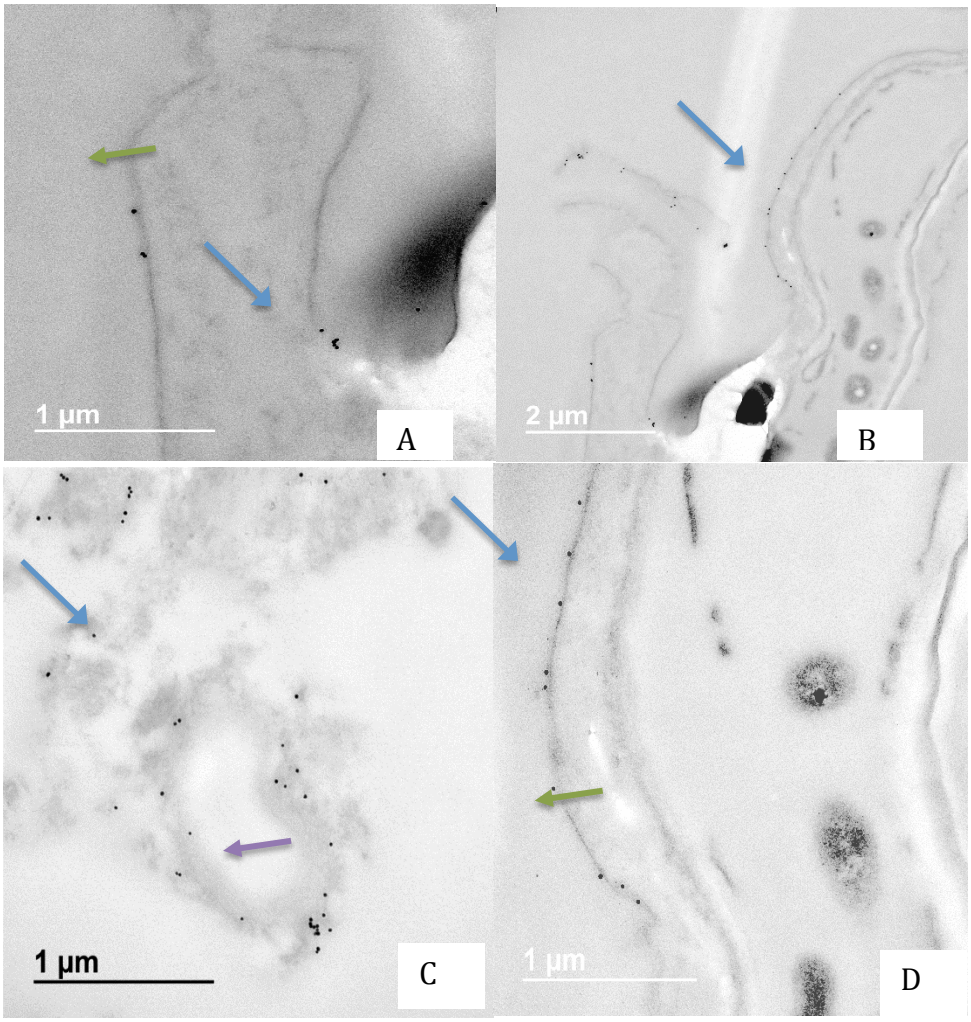

Figure 4-17: TEM images of root samples exposed to 10.0 mg/L 20 nm AuNPs for nine days utilizing LR White Preparation Method. Blue-NPs, Green-Cell Wall, Purple-Vesicle

Figure 4-17 shows TEM images of the root samples created using the LR White preparation method. This preparation method contained no osmium so the outline of organelles and vesicles were not as well defined. However, the images of nanoparticles, when they were found, were clear, sharp and obvious to naked eye. In Plate A, AuNPs can be seen on the outside of the cell wall as well as in plate B. Plate A and plate B are at a magnification of 8,000X and 3,000X respectively. In plate C, at a magnification of 8,000X, AuNPs appeared in the cytoplasm coordinating around a vesicle.

4.2.8 Solution Appearance for Experiment 2

At the beginning of the experiment, all solutions appeared the same color, a light red. However, by the end of the experiment within the same treatment, solutions changed to different colors. These results can be seen in the figure below:

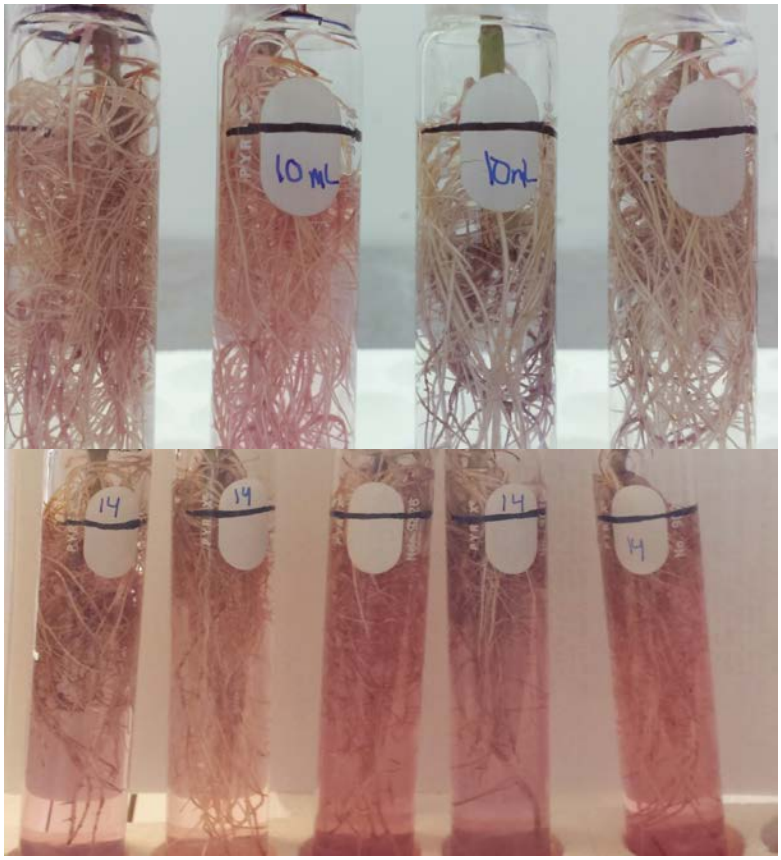

Figure 4-18: Solution appearance of replicates at the end of Experiment 2 (day 9) for both treatments Top photo is for treatment of 10.0 mg/L (n=4) and bottom photo is for treatment of 14.0 mg/L (n=5)

Figure 4-18 shows the appearance of the solutions at the end of the nine day experiment. There was a difference in color between replicates for both the 10.0 mg/L (top photo) and 14.0 mg/L treatment (bottom photo). This was a surprising outcome result and was thought to be a result of the inconsistent dosing and mixing. Because of that reasoning, in Experiment 3, the dosing and mixing was done extra carefully in order to maintain a similarity across all replicates. The results

of the solution appearances were no different and can be seen in the results of Experiment 3 (Section 4.3). A second hypothesis is that the root tissues in each replicate may develop differently (randomly) and, as a consequence, they sorb nanoparticles differentially causing variations in color for the same treatment.

4.2.9 Summary of Experiment 2

From Experiment 2, biomass results at the end of the experiment suggested that the 10.0 mg/L treatment might stimulate sunflower seedlings. However, there was no evidence of a significant difference in transpiration between the controls and AuNP exposure. ICP-MS results showed that no dissolution of Au(III) was detectable, indicating that if NPs were taken up into the plant, they were as AuNPs and not as gold ions. Also, a significant fraction rinsed off, however, the majority of the NPs were tightly sorbed to the roots or uptaken inside the root tissue and the color is still visible with the naked eye. ICP-MS results showed approximately 0.6 mg/L [Au] in the root tissue, however, none appeared to translocate to the stems and leaves. This corroborated with TEM images, which did not show evidence of AuNPs in stems and leaves. According to results from Experiment 2, AuNPs did not significantly translocate but they did sorbed to the roots.

4.3 Experiment 3: Concentration Dependency

4.3.1 Appearance:

Figure 4-19: Photographs of all 4 concentrations (0.0 mg/L, 4.0 m/L, 10.0 mg/L and 40.0 mg/L) Plate A is day 0. Plate B is day 6. Plate C is roots at harvest (8 days). Ascending order for all photos from left to right (0.0 mg/L, 4.0 mg/L 10.0 mg/L and 40.0 mg/L).

Figure 4-19 shows the appearance of *H. annuus* plants during the experiment. Plate A is a picture of the seedlings in hydroponic solution with four different concentrations at day zero. All of the roots were white and fresh in appearance. The color of the solutions range from a light pink for 4.0 mg/L to red for 40.0 mg/L. Plate B shows the plants after six days of exposure. The

solutions changed to be much less colored and the roots became stained somewhat purple (brownish-red). The control roots appeared a little yellow, but they grew during the experiment and appeared healthy. The other root treatments also grew, and the colors changed from pink to purple hue during the course of the experiment. Plate C provides a photo of the roots at harvest and the roots are shown in ascending order from left to right (Control, 4.0 mg/L, 10.0 mg/L, and 40.0 mg/L). The 4.0 mg/L roots appeared light purple, the 10.0 mg/L roots appeared a light pink and the 40.0 mg/L roots appeared a dark purple.

4.3.2 Biomass

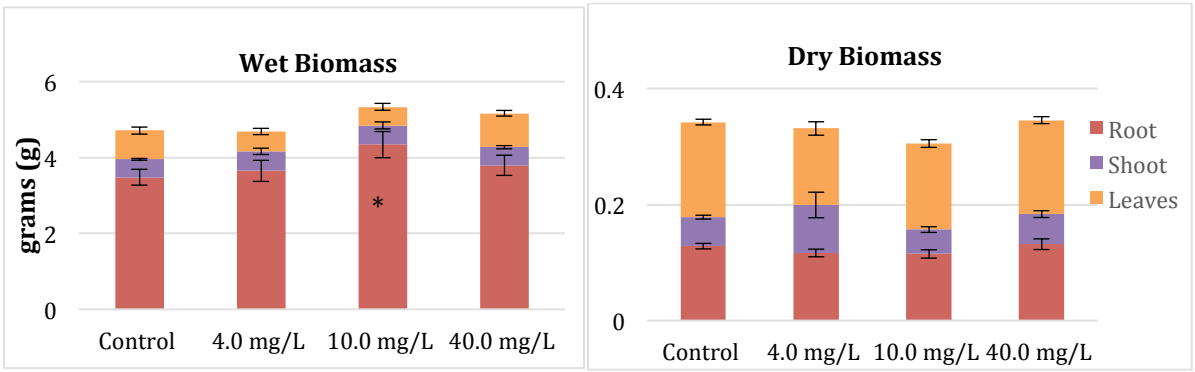

Figure 4-20: Wet biomass(left) and dry biomass(right) of four exposure concentrations to 20 nm AuNPs after eight days. Control (n=7) and for treatments (n=6).

Figure 4-20 shows the wet biomass (Left) and dry biomass (Right) of the roots, shoots and leaves for all four treatments in experiment 3 at harvest (eight days). Overall, there was not a significant difference in biomass among treatments versus the control. Total biomass at the end of the experiment was almost equal in all cases at approximately 5 grams. However, the wet plant biomass in roots for the 10.0 mg/L treatment versus the control indicated a statistical significance (p- value 0.048). This is likely due to random variations among seedlings and only occurred in the wet biomass root measurements, and not for dry biomass. It is unlikely that the

10.0 mg/L treatment was stimulatory compared to the controls and it is concluded here that the treatments were neither inhibitory nor stimulatory to exposure of AuNPs.

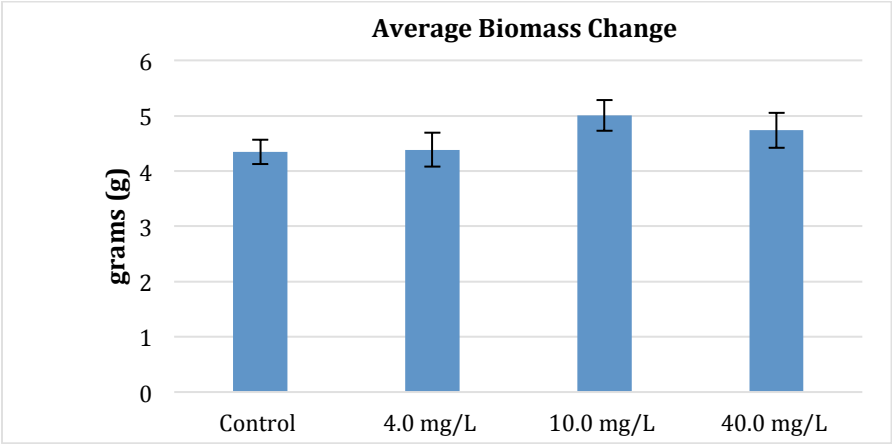

Figure 4-21: The biomass change over twelve days from initial transplantation to harvest with eight days of exposure to 20 nm AuNPs.

Figure 4-21 shows the growth in biomass overall. The initial biomass was taken at the day of transplanting, and the plants were allowed to adjust to their new environment for 5 days, and then they were exposed to nanoparticles for 8 days. Overall Figure 4-21 shows that gold nanoparticles had no significant effect on overall sunflower growth. All the plants in each treatment grew approximately the same amount, between 4-5 grams in a 12 day period. The treatment at 10.0 mg/L in Figure 4-21 appears to be greater than the control, however, this was not statistically significant (p-value 0.52). In conclusion, all plants exposed to nanoparticle treatments showed equal, vigorous growth during the experiment and the growth was approximately equal to the growth exhibited by the controls.

4.3.3 Transpiration

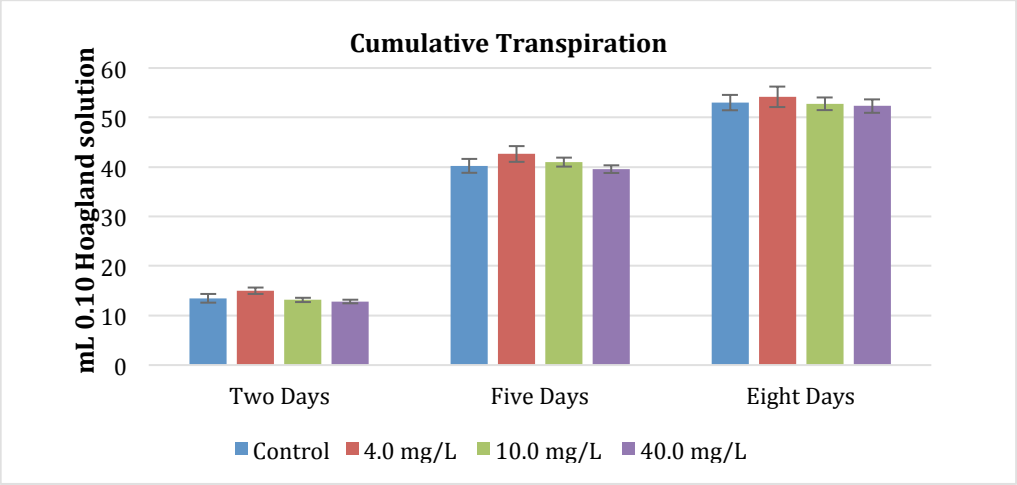

Figure 4-22: Cumulative transpiration over eight -day exposure of 20 nm AuNPs. Control (n=11), 4.0 mg/L (n=8), 10 mg/L (n=6), 14.0 mg/L (n=6).

Figure 4-22 shows the cumulative transpiration during the eight -day exposure. Overall, the controls and all the treatments were transpiring vigorously during the experiment. There were significant differences between the transpiration of plants at each time point (2, 5 and 8 days), but there were no significant differences between treatments within each time point. Exposure of the seedlings to nanoparticles at various concentrations did not inhibit or stimulate cumulative transpiration. These results are in good agreement with the results from the biomass growth measurements in Figure 4-20 and 4-21, and indicate that the nanoparticle concentrations were not interfering in transpiration of the sunflower seedlings during the course of the eight day experiment.

4.3.4 ICP-MS Solutions

The concentration of AuNPs in unfiltered solution samples decreased over time during the experiment. One mL samples of the solution were taken on day zero, day two, day five and day eight in order to see the decrease of [Au] in solution. Figure 4-23 shows the results of [Au] in

solution over time. The concentration values on Day 0 were always less than the targeted dose and this difference is a measure of the rapid sorption that occurred within a couple of hours after introducing the nanoparticles to the solution containing the sunflower roots and seedlings. For example, the concentration at Day 0 in Figure 4-24 for the 40.0 mg/L treatment was 27 mg/L indicating a rapid loss of approximately 13 mg/L from the targeted dose. This demonstrate that sorption of gold nanoparticles to roots is quite rapid.

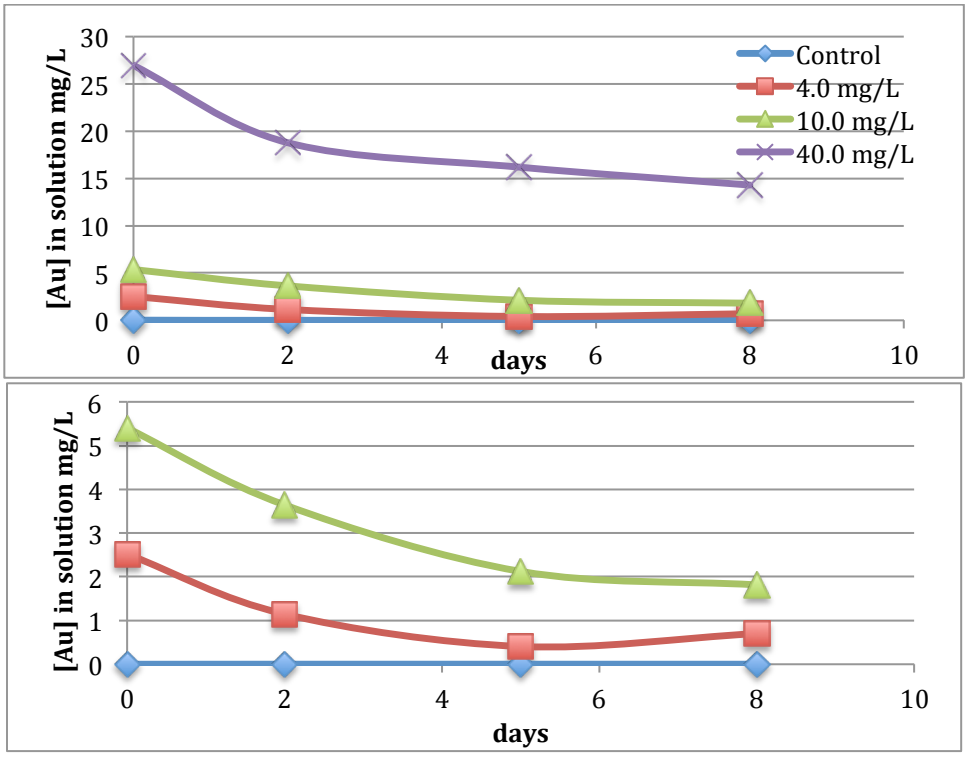

Figure 4-23: Au concentration (mg/L) in solution over eight days of the experiment as a function of various nanoparticle concentrations.

Figure 4-23 shows the Au concentration over 8 days with an expanded y-axis (top) and a finer scale (bottom). From the bottom figure, the 4.0 mg/L treatment seems to increase in concentration on day 8 while the other two treatments continue to decrease. This is an unlikely result and the data point for the 4.0 mg/L treatment on day 8 was disregarded. From the ICP-MS

analyses, a rate constant of sorption (loss from solutions) can be estimated for each treatment. In order to do this [Au] solutions were normalized (C/C_0), and a slope and R^2 value were determined. The results are below:

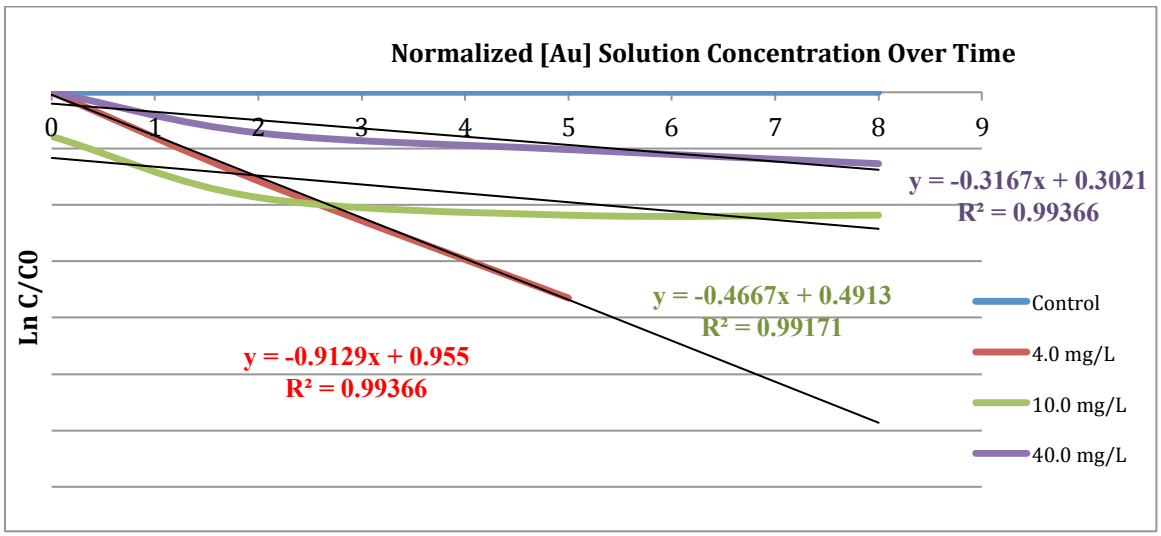

Figure 4-24: Normalized [Au] concentration over eight day exposure period to 20 nm AuNPs. Blue line- 0.0 mg/L Purple-40.0 mg/L Green-10.0 mg/L and Red-4.0 mg/L.

Figure 4-24 shows the normalized [Au] solution concentration with time. A rate constant (k) of sorption of 20 nm Au NPs was found for all three treatments. The 4.0 mg/L treatment had the highest sorption rate constant with a slope of 0.913 day^{-1}. The 10.0 mg/L and the 40.0 mg/L had a similar slope or rate constant of 0.317 and 0.467 per day respectively. The smallest concentration had the greatest loss/sorption rate constant and the largest concentration had the smallest indicating that it is not truly a first order rate constant (the rate constant is not constant).

The test tubes containing the solutions and seedlings were inverted ten times every day in order to provide oxygen to the cells from the headspace. Perhaps, some nanoparticles agglomerated and settled to the bottom (although only some were observed at the bottom at the higher treatment concentrations) and, thus, the nanoparticles were not as available for sorption

with the roots as the lower concentration treatment. With mixing ten times per day, the AuNPs in all treatments were intermittently re-suspended but the higher concentrations of AuNPs were not available to the roots as completely as the nanoparticles at the lower concentration treatment.

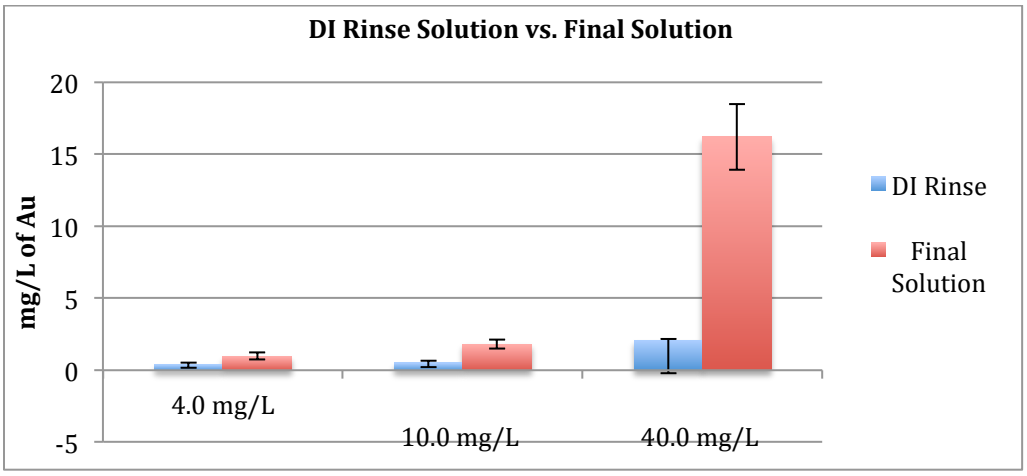

Figure 4-25: ICP-MS [Au] of Rinsed roots versus un-rinsed roots

Figure 4-25 shows the concentration of nanoparticles that came off during the rinse process compared to the amount in the solution at the end of the experiment. During the rinse process, roots were placed in a clean test tube and rinsed with DI water. The greatest difference was clearly at the 40.0 mg/L concentration. The amount of nanoparticles that came off during the rinse process was significantly less than amount of nanoparticles in solution. Nanoparticles seemed to have sorbed somewhat more strongly during Experiment 3 than Experiment 2 as measured by the difference in the rinsed solution versus the original solutions. Despite the variability between experiments, it was clear that NPs readily desorbed during the rinse process while some remained tightly bound in or on the roots. Overall, the AuNPs were sorbed to the roots quickly (but not strongly) and were liberated by a simple rinsing with DI water.

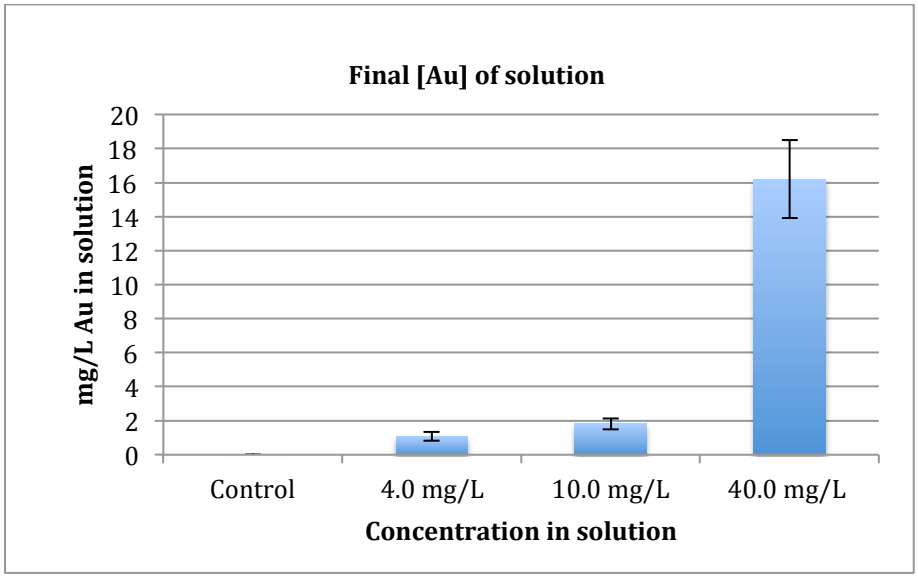

Figure 4-26: Final [Au] concentration in solutions after eight day exposure to 20 nm AuNPs.

Figure 4-26 shows the final Au concentration after eight days between treatments. As shown in Figure 4-26, all three concentrations have less than half of their original dosed concentration after eight days. The percent difference between the initial dosed concentration and the final for 4.0 mg/L, 10.0 mg/L, and 40.0 mg/L are the following: 73%, 82% and 59.5% respectively. The nanoparticles disappeared from solution by sorption to roots as confirmed by the rinse process and by the measured final concentration on the roots (Figure 4-28). The control, without the addition of AuNPs consistently registered no detectable Au counts in ICP-MS analyses, which is another measure of quality assurance.

4.3.5 ICP-MS Plant Tissue

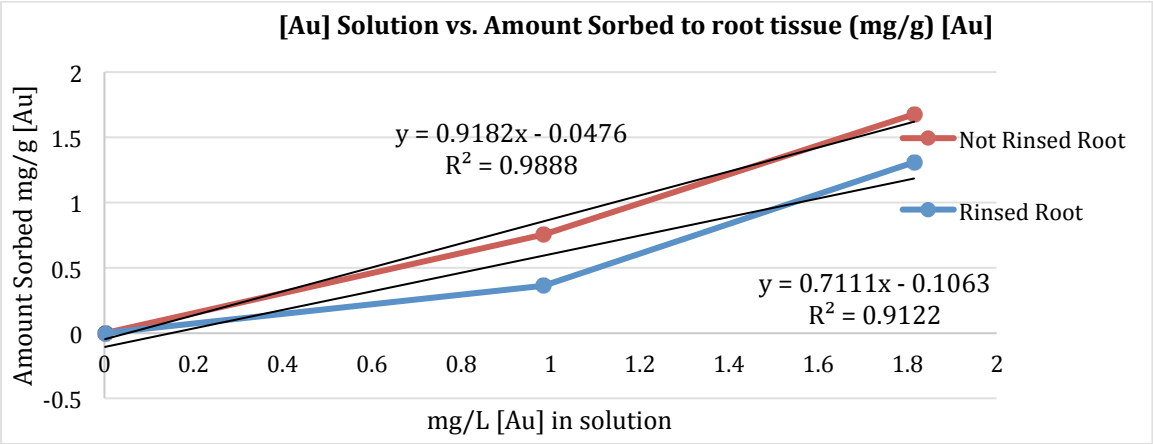

Figure 4-27: ICP-MS of root tissue in Experiment 3 for the following treatments after eight days: 0.0 mg/L, 4.0 mg/L, and 10.0 mg/L treatments.

Isotherm Experiment. Figure 4-27 shows the ICP-MS results of [Au] in solution versus the amount of [Au] in root tissue that was rinsed and not rinsed in Experiment 3. Figure 4-27 shows the results for solution and root tissue for the following treatments: control, 4.0 mg/L and 10.0 mg/L. From Figure 4-27, a Kd value can be estimated for both the rinsed and not-rinsed root solutions. The slope for the not-rinsed roots in Experiment 3 was 0.9182 L/g or 918.2 mL/g. The Kd estimation for AuNPs that were not as strongly sorbed to the roots was 711.1 mL/g. These results showed that more NPs sorbed to the roots do wash of which corresponded to results found in Experiment 2. Next, a membrane uptake efficiency can be calculated using the following equation:

Membrane uptake (mg/day)= efficiency * Transpiration rate (mg/day) * C_{NP} (mg/L)

The membrane uptake efficiency is expected to be zero because AuNPs were never clearly evident in stem tissue data for TEM images. However, according to the ICP-MS results, a small fraction bypassed the membrane. The cumulative transpiration rates per eight days for

experiment 3 were 6.78 mL/day, 6.60 mL/day and 6.54 mL/day for 0.004 mg/mL, 0.01 mg/mL , and 0.04 mg/mL treatments respectively.

Table 4-1: Membrane uptake efficiency for roots

Rinsed Roots Treatment	Uptake mg/day	Transpiration Rate (mL/day)	Cnp (mg/mL)	efficiency
4.0 mg/L (n=3)	0.0031	6.7722	0.0040	0.1145
10.0 mg/L (n=3)	0.0110	6.5950	0.0100	0.1670
40.0 mg/L (n=2)	0.0279	6.5375	0.0400	0.1068

Table 4-1 shows the required data and resultant efficiency calculation for the membrane uptake efficiency of AuNPs in *H. annuus* seedlings. The rinsed roots were used for the membrane efficiency calculation because those are where the gold is expected to have sorbed and bypassed the cell membrane. According to Table 4-1, the root membrane efficiency to is approximately 10-17%. In other words, 11-17 NPs bypass the cell wall and membrane for every 100 individual NPs. This is not a great efficiency, indicating that the sunflower seedling membrane and cell wall do a pretty good job of distinguishing them as not a required nutrient. However, Au is still able to bypass the cell wall and membrane, and the exact mechanism is still unclear. The efficiency seems to increase from 4.0 mg/L to 10.0 mg/L, but then decreases at the 40.0 mg/L concentration. This could be a random result due to the lower number of replicates for the 40.0 mg/L (n=2). Also this could be a result of a variation with the ICP-MS.

QA/QC. Looking at all the information provided in Figure 4-23 to Figure 4-27, an approximate mass balance for Au was estimated. The mass balance calculation used for the 10.0 mg/L treatment and 4.0 mg/L treatment are:

$$M_{\text{rinsed root tissue}} + M_{\text{root tissue}} + M_{\text{DI rinse water}} + M_{\text{solution}} + M_{\text{day 2}} + M_{\text{day 5}} = 10 \text{ mg/L (0.05 L)}$$

The mass of Au in the root tissue in the 10.0 mg/L treatment for DI rinse and final solution were 0.088 mg and 0.058 mg respectively. The concentration of Au in the original solution and the DI rinse are 0.09 mg and 0.025 mg respectively. Finally two 1 mL samples were taken out of the system on day 2 and day 5 and their masses are 0.00365 and 0.00212 mg respectively. Adding all of these values equals 0.267 mg, which means that the mass balance does not agree. The left side of the equation only accounts for approximately 54% of the original dosed value. Only 54% of the initial dosed gold is found to have sorbed/uptaken into the roots. The mass balance was repeated for the 4.0 mg/L treatment with a result 64%. Overall, the mass balance at both treatments (4.0 mg/L and 10.0 mg/L) were missing a significant amount of the initial dosed gold. Including the gold found in the stem and tissue data do not aid in this discrepancy (Figure 4-28 and 4-29). As a result, the mass balance discrepancy is suspected to be a result of the AuNPs accumulating at the bottom of the test tubes or sorbing to the glassware. This theory could explain why there was less of a difference in the 4.0 mg/L treatment compared to the 10.0 mg/L treatment. Other suggestions could be due to the variations in the ICP-MS results or loss of NPs during the inversions/shaking of the test tubes. Upon re-examination of the test tubes, aggregated NPs were visually seen accumulating at the bottom of the test tube (See Appendix Figure A-9). The deposits of gold NPs at the bottom are suggested to account for approximately the other 40% of Au.

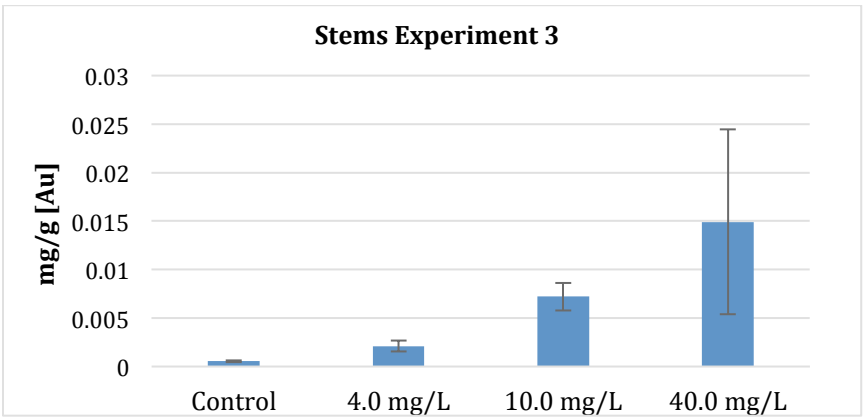

Figure 4-28: ICP-MS [Au] of shoot tissue in Experiment 3 after eight-day exposure.

Figure 4-28 shows ICP-MS results for stem tissue from Experiment 3. No spiked gold was added and a clear correlation can be seen between stem [Au] and AuNP exposed concentration. There is no statistical difference between 40.0 mg/L compared to the control with a p-value of 0.27.

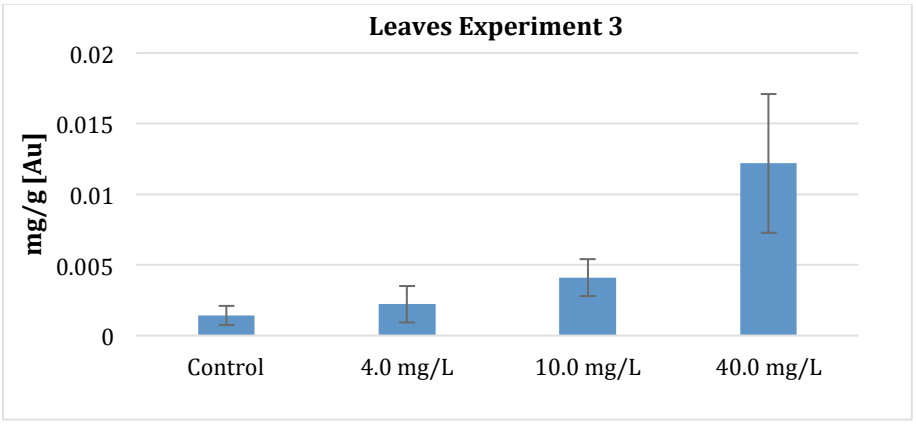

Figure 4-29: ICP-MS [Au] of leaf tissue in Experiment 3.

Figure 4-29 shows the ICP-MS results for concentration of [Au] in leaf tissue. The results show a similar increase with concentration as shown in Figure 4-28. Compared to Experiment 2, there was a lot less gold and is likely a result of the no spiked addition. There was no statistical difference between 40.0 mg/L and the control with a p-value of 0.09. Despite this, there does

appear to be a linear relationship between concentration and [Au]. Although not a statistically different amount, NPs do appear to get into leaf tissue.

4.3.6 Appearance of Solutions for Experiment 3

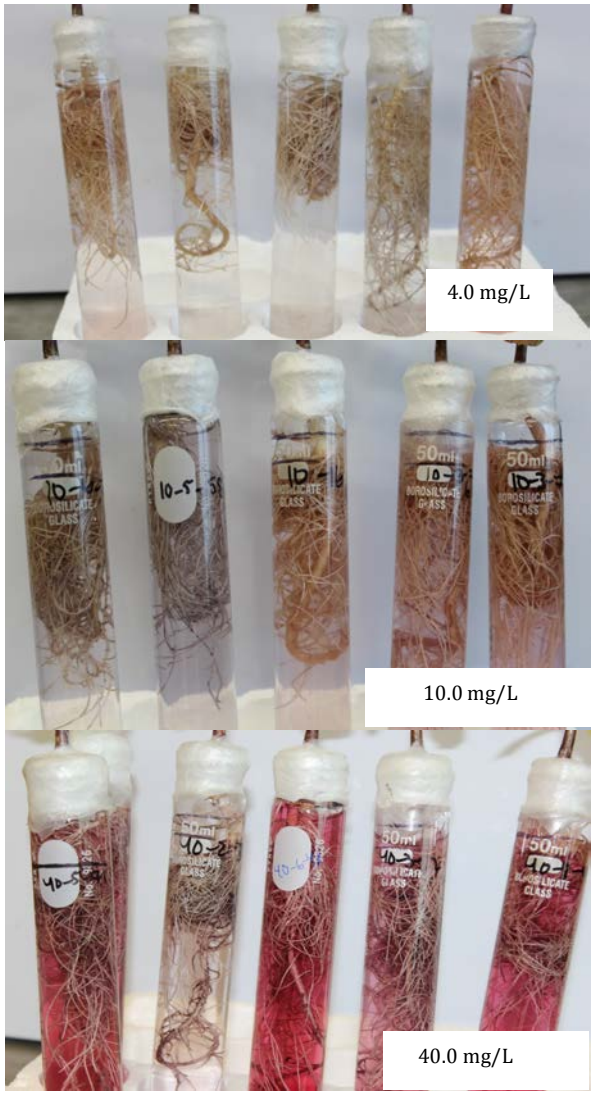

Figure 4-30: Appearance of solutions after eight-day exposure to 20 nm AuNPs of three different concentrations(4.0 mg/L, 10.0 mg/L, and 40.0 mg/L).

Figure 4-30 shows the appearance of the solutions and roots of the three different treatments on day eight (n=5 replicates in each photo). The top photo represents 4.0 mg/L. In the top photo, the three middle replicates appear to be a clear to a light purple, however, the two outermost test tubes have a solution with a slightly more evident light pink color. The middle

photo was of sunflower seedlings in the 10.0 mg/L of 20 nm Au NPs. The test tube on the left appears clear, and the solution colors ranged from purple to a light pink. On the bottom photo, a 40.0 mg/L treatment, colors varied from a deep dark pink to a light purple for the 5 replicates. The same change in solution color in similar replicates was also observed in Experiment 2. Because of the variability in color observed in Experiment 2 (Figure 4-18), particular care was taken to introduce the nanoparticles uniformly in Experiment 3 (Figure 4-30). The nanoparticles were carefully measured out and administered into each test tube.

The results in Figure 4-30 showed that despite having the same concentration, the roots interacted with the NPs differently. A purple solution color is known to represent aggregated nanoparticles (McFarland, 2004). However aggregation, apparently, did not occur equally in every replicate. Although the solution only turned purple in a few replicates, it was very common to see the roots turn a purplish color as the NPs began to aggregate on the roots. Despite the solution changing colors within replicates for the same treatment, it was apparent throughout all treatments that NPs were sorbing to the roots. Especially in the 40.0 mg/L treatment, the dark appearance of the roots showed an accumulation of NPs on the surface of the roots apparent to the naked eye. Ultimately, it is suggested that the various color changes were dependent upon how the roots "accepted the stain" of gold nanoparticles. Different seedlings developed different root tissue textures (a natural biological variability), which sorbed the AuNPs differently. More studies on the various sorptive effects on root tissues could help us better understand the relationship between nanomaterials and roots.

4.3.7 Summary of Experiment 3

In summary, Experiment 3 showed no evidence of phytostimulation or phytotoxicity based on measurements of biomass growth or cumulative transpiration. There was a significant

uptake/sorption of AuNPs onto roots that could be seen with the naked eye and measured by ICP-MS. A large fraction of these sorbed nanoparticles could be rinsed from the roots with a simple DI rinse. Sorption to roots was rapid, but most of the sorbed nanoparticles could be removed from the outside of roots by a light rinsing.

4.4 Experiment 4: Nanorods vs. nanoparticles toxicity to sunflower

4.4.1 Appearance of seedlings of Experiment 4

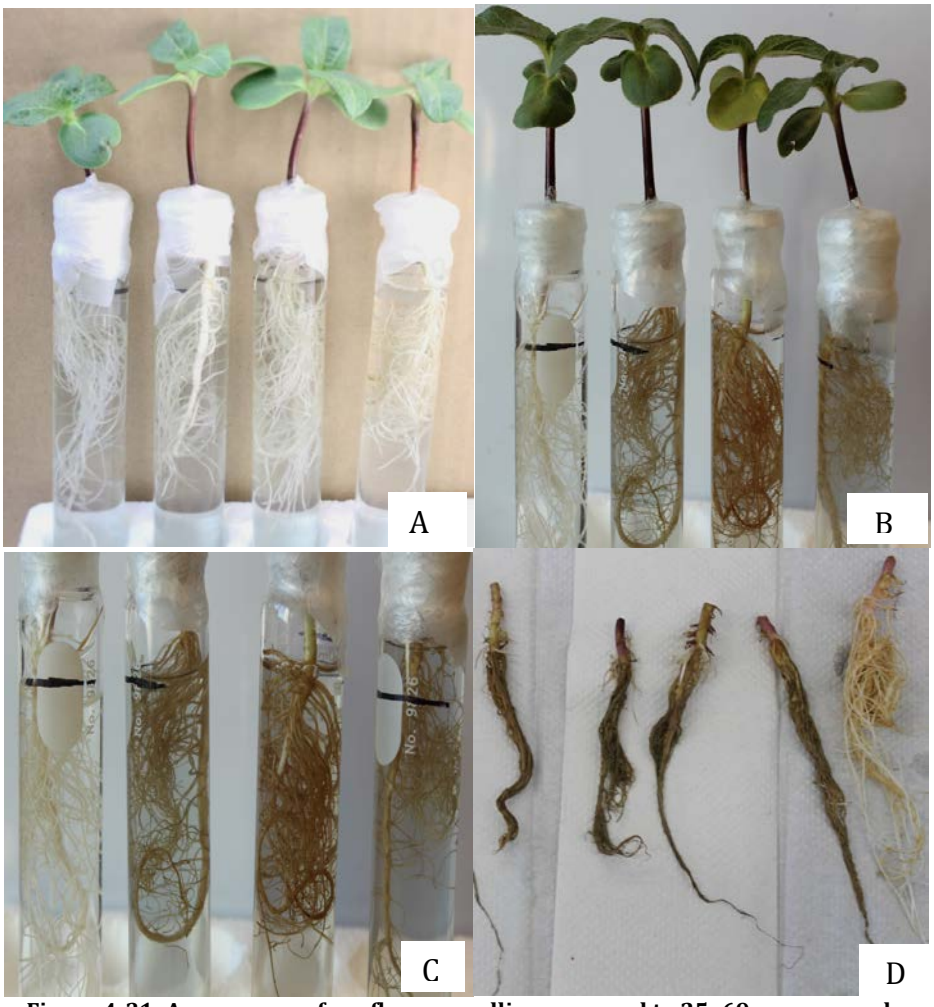

Figure 4-31: Appearance of sunflower seedlings exposed to 25x69 nm nanorods.

Figure 4-31 shows photos of Experiment 4. The purpose of Experiment 4 was to study the exposure of gold nanorods (of similar size but different shape and surface charge) to sunflower

seedlings and to compare them to nanoparticles. As shown in figure 4-31, Plate A is a photo of *H. annuus* seedlings dosed with nanorods on day zero. All the roots appeared to be white and the solutions were a light blue. Plate B was taken after two days of exposure. The test tube on the left is the control for comparison and the roots for the control appeared white. The other three treatments in Plate B turned a dark brown after two days. The sunflower seedlings appeared to stay green, however their roots eventually died. Plate C is a close-up of Plate B emphasizing the two-day change in root color. Finally, Plate D shows the roots after harvest on day 8 when the roots appeared black, mushy and dead compared to the control (far right). The leaves of the seedlings did not change drastically during the eight days, they stayed green, however, with the biomass results, it is clear that they stopped growing when exposed to nanorods. In conclusion, it is suggested that death was caused by toxicity within the root system.

4.4.2 Biomass

After eight days of exposure, the biomass of the plants exposed to 6.0 mg/L of Au 25x69 nm nanorods were collected and compared to the eight-day exposure of 10.0 mg/L of 20 nm Au NPs and control plants. The total final biomass and the biomass change from the time of transplantation to harvest are shown in the next two figures. The sample size for the control treatment (n=7), 10.0 mg/L treatment AuNPs (n = 6), and for 25x69 nm nanorods treatment (n=5).

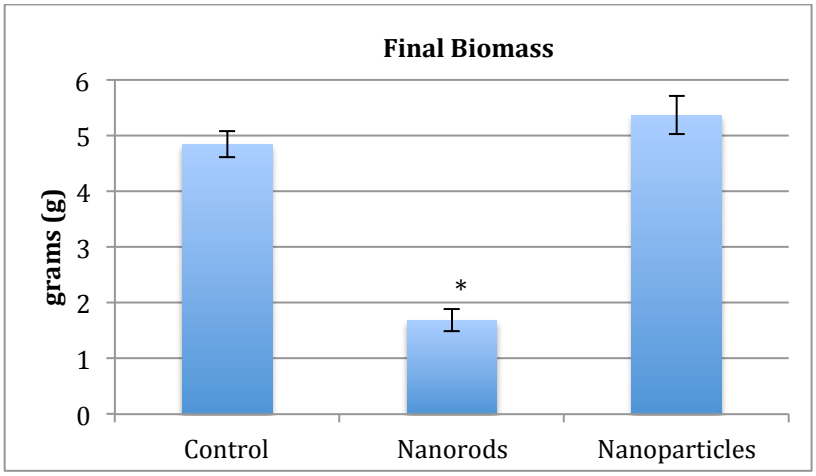

Figure 4-32: Final biomass after eight days for 0.0 mg/L, 6.0 mg/L, and 10.0 mg/L.

Next, biomass change over time was plotted in Figure 4-33. The plants were initially weighed during transplanting then allowed to adjust to their surroundings for six days and exposed to 6.0 mg/L of nanorods (initial concentration) for eight days. The control (n=5) and nanoparticles (n=6) values were taken from experiment 3 and the middle bar graph shows the results of 6.0 mg/L treatment of 25x69 Au nanorods exposed to 5 sunflower seedlings (n=5).

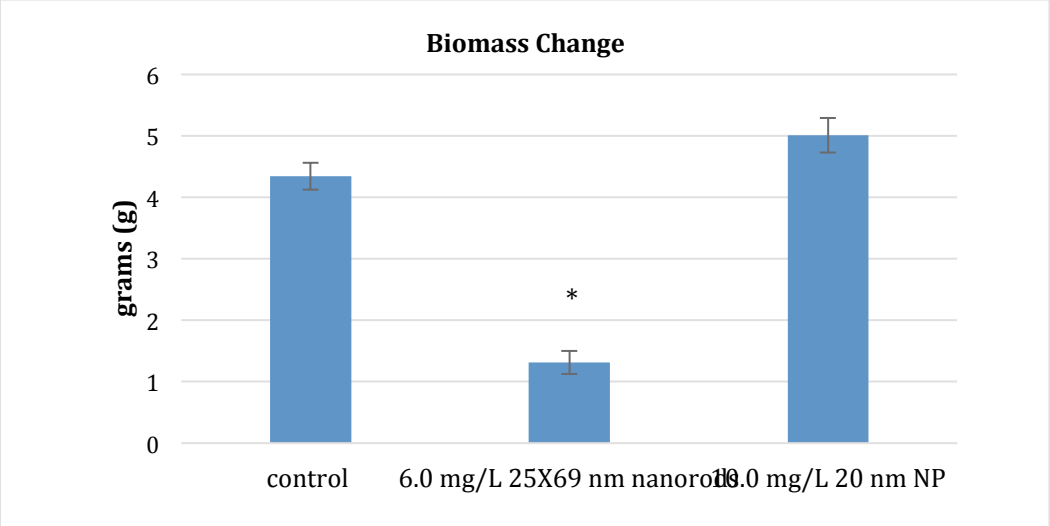

Figure 4-33: Change in biomass from transplant to harvest (14 days) for plants exposed to 25x69 nm Au nanorods for eight days.

It is clear from Figure 4-32 and 4-33 that nanorods had a huge impact on the health of sunflowers. Even after two days of exposure, they stopped growing and the roots immediately turned brown (See figure 4-31). Figure 4-33 shows the biomass change. Even when comparing, 6.0 mg/L nanorods to 10.0 mg/L nanoparticles, one can see that nanorods had a huge impact on sunflower's ability to grow and survive. Conducting a t-test between the treatments exposed to nanorods and the control the p-value was $4.78 * 10^{-6}$. Overall, the seedlings exposed to nanorods only grew because they were allowed to adjust to their new surroundings without nanorods for five days. After exposure, to 25x69 nm Au nanorods, their roots turned black and they died quickly.

4.4.3 Transpiration

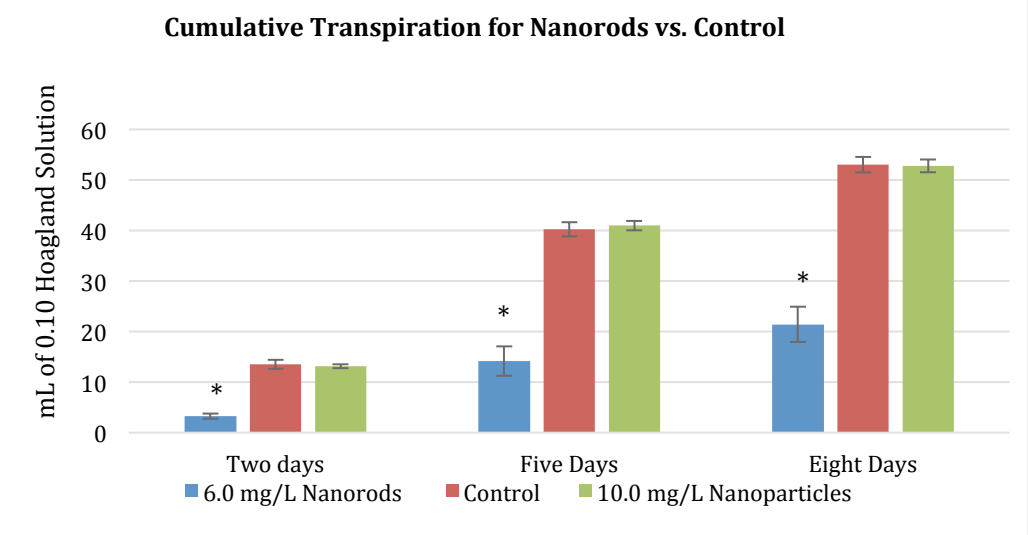

Figure 4-34: Cumulative Transpiration of eight day exposure to 25x69 nm Au nanorods compare to control and 10.0 mg/L 20 nm AuNPs.

Figure 4-34 shows the overall transpiration compared to transpiration of seedlings that was exposed to 10.0 mg/L of Au nanoparticles (20 nm) and the control. For each day there was a statistically significant difference in transpiration between plants exposed to nanoparticles and plants exposed to nanorods. The p-values are all in the 10^{-6} range for day two, day five, and day eight. There was no statistically significant difference between Au nanoparticles and control, however, there was statistically significant difference when comparing nanorods. This corroborated with biomass data and suggested that nanorods were statistically more phytotoxic than nanoparticles and completely inhibited both transpiration and growth at 6.0 mg/L.

4.4.4 Summary of Experiment 4

As a result of this study, AuNPs could be considered as a potential candidate for targeted gene delivery in developing plant root systems. On the other hand, nanorods would not be a good

candidate. However, more research needs to be done on what characteristics of nanorods make them more toxic. As described in the literature review, the gold nanoparticles used in this study were citrate stabilized and the citrate provides a negatively charged surface. The gold nanorods are CTAB stabilized and this corresponds to a positively charged surface. A positively charged surface was discussed in the literature review as more likely to be attracted to the negatively charged cellular membrane. Therefore, the CTAB surface coating is expected to be the main cause of the plant toxicity and is toxic to both to *H. annuus* and maize seedlings (Moradi, 2014).

4.5 Experiment 5: Sorption

4.5.1 Kd estimation

In experiment 5, roots were completely immersed in 50 mL test tubes in 5 different concentrations (0.0-15.0 mg/L) of 20 nm Au NPs. They were placed on a mixer for four hours then the roots were dried. The solutions and the roots were measured using ICP-MS. From these results an absorption curve is created and a Kd value can be estimated:

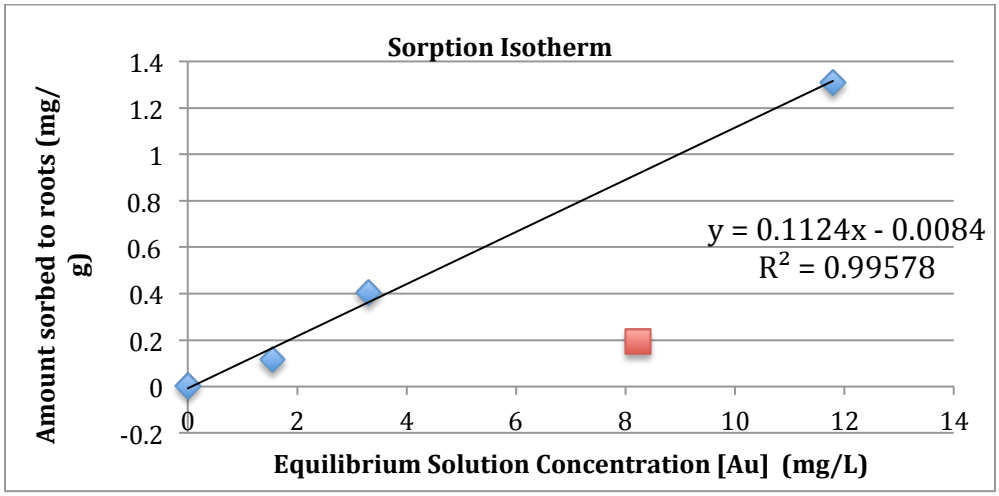

Figure 4-35: Kd estimation of 20 nm AuNPs to H. annuus roots.

Figure 4-35 shows the sorption isotherm after 4 hours of equilibrium . The slope represents the Kd (sorption value) of AuNPs to roots after 4 hours at 885.8 mL/g . This value corresponds to previous estimates of the Kd from Experiment 3. (See 4.3.5). The Kd value for experiment 3 over 8 days is approximately 9,182 mL/g. These values are extremely similar and show that equilibrium between roots and AuNPs occurred quickly. The red square in Figure 4-35 represents an outlier that was removed because it was approximately greater than two standard deviations away. The outlier occurred at 10.0 mg/L treatments and was not included in the Kd estimation. This Kd value is very high and shows that AuNPs are highly sorptive to roots.

A mass balance can also be conducted on this experiment. In this experiment, there were no samples taken throughout the duration of the experiment and the roots were not rinsed. Therefore the mass balance is the following:

$$M_{roots} + M_{solution} = \text{Total Mass of [Au]}$$

For Experiment 5, the percent recovery was calculated for the following concentrations: 2.0 mg/L, 5.0 mg/L, and 10 mg/L. The following percent recovery is 84%, 75%, and 87% respectively. The percent recovery for this experiment was significantly greater than the mass balance in experiment 3. The increased percent recovery is expected to be due to the decrease in variables that could have caused a loss of Au as well as the time duration of this experiment. Experiment 5 was only run for four hours while Experiment 3 was over the duration of 8 days. In addition, Experiment 5 took place on a shaker, which kept the nanoparticles well mixed in solution, and unable to aggregate and fall to the bottom as is expected to have occurred in Experiment 3. There is still approximate 20% of Au missing and this is expected to be sorbed to the glassware.

4.5.2 Summary of Experiment 5

Estimating the Kd values puts a mathematical value of AuNPs sorbtivity to roots. This allowed an understanding and way to characterize its ability to be used as an application. First the Kd value from experiment 3 is 918.2 mL/g and the Kd value from Experiment 5 was approximately 112.4 mL/g. The discrepancy between the Experiment 3 Kd value and the Experiment 5 Kd value was a result of Experiment 3 was still growing and the sorption sites were still being created. Since the Kd value is a lot higher than 5, it can be deduced that AuNP will highly sorb to organic material and will not move throughout the soil. In addition, it might be hard to use AuNPs for targeted gene delivery applications because if applied to non-hydroponic situations, the NPs will never make it to the roots and stick to the soil. Figure 4-36 shows a linear isotherm relating AuNP sorption to roots. Experiment 5 had a greater percent recovery and the missing [Au] in the mass balance is expected to have sorbed to the glassware.

Chapter 5 Conclusions

1. From experiment 1, the temperature did not have a significant impact on nanoparticle uptake possibly suggesting that endocytosis is not a predominant mechanism. Some particles entered the cytosol at both temperatures as evidence by TEM imaging (Figure 4-4 and Figure 4-5 in Section 4.1.2)
2. *H. annuus* exhibited no phystostimulation or phytotoxic effects when treated at a range of AuNPs (20 nm average spherical diameter). When seedlings were exposed to 3.0-40 mg/L, no phyto-effect occurred. These results suggest that gold nanoparticles stabilized with citrate are relatively inert with respect to sunflower seedlings growing in hydroponic solutions. This is likely due to the negatively charged surface coating from citrate that is repelled from the plant cell membrane but did not cause a phyto-effect. Despite repulsive forces, TEM images and ICP-MS did confirm that AuNPs bypass the cell membrane. See section Sections: 4.1.2, 4.2.2, and 4.3.2.
3. There was no significant uptake or translocation of NPs into the shoots and leaves of sunflower seedlings in hydroponic solution (See Sections 4.2.6 and 4.3.5). A Kd value was for AuNPs sorption to roots was found as 915.8 mL/g. For tightly sorbed nanoparticles, the Kd value was estimated at 711.1 mL/g. In addition, Table 4-1 shows a membrane efficiency for the root cells to be approximately 10-17%.
4. There was significantly lower biomass in sunflower seedlings upon exposure to gold nanorods when compared to gold nanoparticles (Section 4.4) indicating some toxicity of the nanorods to root tissues. This is likely due to the cationic coating of the nanorods by CTAB, which is a known antiseptic agent for bacteria and fungi.

5. The mass sorbed relative to nanoparticle concentration in solution shows a linear isotherm and can be seen in both Experiment 3 and Experiment 5. The estimated Kd value in Experiment 5 was 885.7 mL/g. (Sections 4.3.5 and 5.3.1)

Chapter 6 : Future Work

Future studies could be done to further identify why the solutions varied in their change in color. This could help enlighten specific nanomaterials interactions with roots. What about the root architecture is the driving force that caused gold NPs to aggregate differentially? Is it root exudates, the smaller roots, the primary root, or just how the roots are situated in the test tube that ultimately caused the varied color changes? Other work with nanoparticles and plants would be to attempt to identify the specific mechanism by which these man made materials transport into plants cells. In addition, as they transport into the cell, physically identify where they accumulate in the plant cells and why do they accumulate in the cell. Taking the idea of nanoparticles with sunflower further is to see if nanoparticles could be passed onto next generation from seed to seed. This work focused primarily on the early vegetative stage and not on any reproductive stages. Since a major portion of the sunflower cash crop are the seeds, it is important to understand if there are potential toxicity risks for NPs to accumulate in the seed of sunflowers. Although, AuNPs were not toxic, Au nanorods were toxic. Nanorods were significantly more phytotoxic than nanoparticles. This was surmised to be a result of their surface charge and was not a result of their different shape. It would be beneficial to study two differently shaped nanomaterials with the same surface charge to see if the difference is solely surface coating dependent. In addition, future research can identify the mechanism at which both nanorods and nanoparticles enter *H. annuus*. Studying other nanoparticles that are more likely to be found in the environment such as CeO_2, TiO_2 and AgNPs might be beneficial because these are the ones that are more likely going to accumulate in natural environments.

Appendix

FigureA-1: A photo of the separate part of the sunflower that were tested for biomass and ICP-MS of the roots stems and leaves.

Figure A-2: Photos from the sorption experiment (Experiment 5). On the left are the capped roots from ascending concentration order from left to right: 0.0 mg/L, 2.0 mg/L, 5.0 mg/L, 10.0 mg/L and 15.0 mg/L. The right photo shows the test tubes on the shaker.

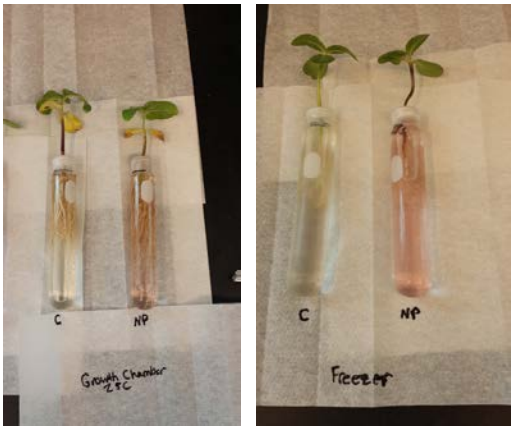

Figure A-3: Experiment 1 visual results. Picture on the left and the right both show the increased biomass in the warmer temperatures and the root color of roots exposed to 3 mg/L of nanoparticles.

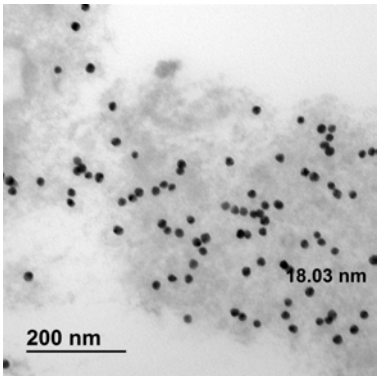

Figure A-4: TEM image of nanoparticles found within cytoplasm of the cell. This picture is very similar to Figure 1-4 and corroborates the thinking that these nanoparticles are found in day 2 root tissue at 7.5°C.

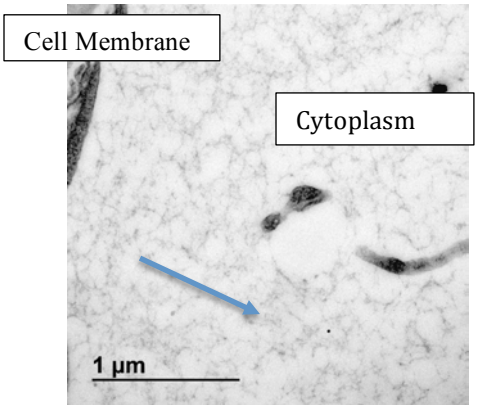

Figure A-5: 8,000X Magnification for TEM. There might be one in lower corner. The nanoparticle appears dark and electron dense. These sightings were very rare within the shoot and leaf samples. This photograph was taken from a stem at 14.0-mg/L exposure of 20 nm Au NPs over nine days.

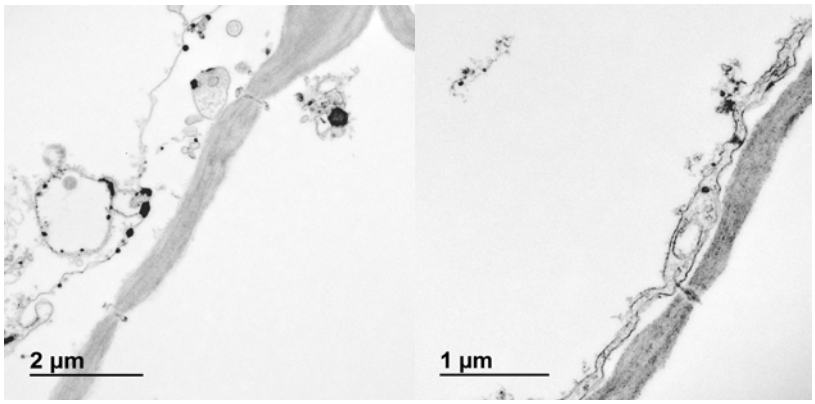

Figure A-6: Left is 14 mg/L roots after nine days at 3,000 X magnification. On the right is 14 mg/L root after nine days at 6,000 X magnification. Both contain electron dense round circular shapes, however, taking these images and comparing to visuals we found in figure 8-5, it was decided that samples might appear better utilizing another TEM preparatory method.

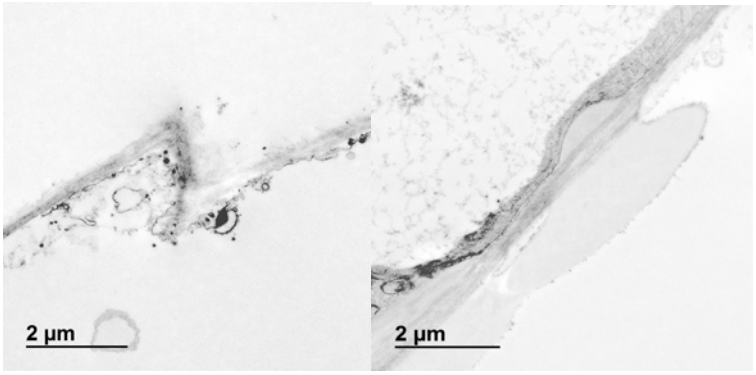

Figure A-7: TEM images that were prepped using Osmium. Control roots at 3,000X look similar to the roots at 14 mg/L. Dark circular electron dense shapes appear along cell membrane. As a result, another preparation method without Osmium was used and analyzed.

Figure A-8: Bottom of 10 mg/L test tube from Experiment 3. The unaccounted for Au is expected to have accumulated at the bottom of the test tube or sorbed to the glassware.

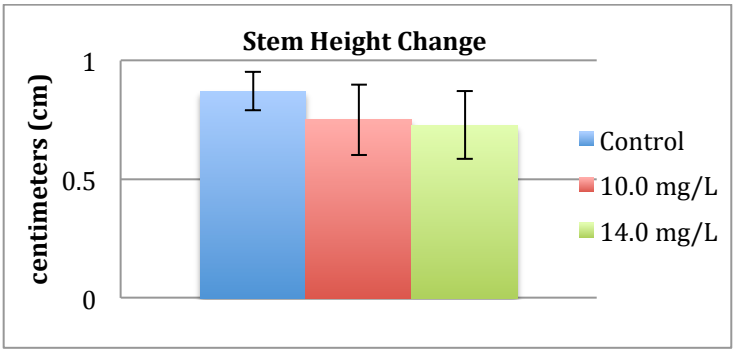

Figure A-9: Estimated change in stem height during nine-day exposure from Experiment 2.

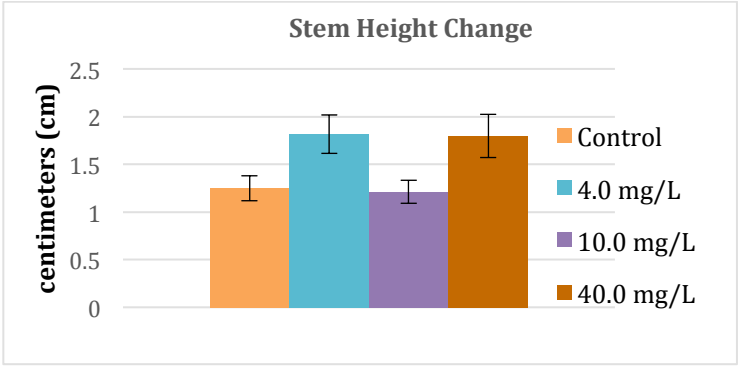

Figure A-10: Estimated stem height during eight-day exposure from Experiment 3.

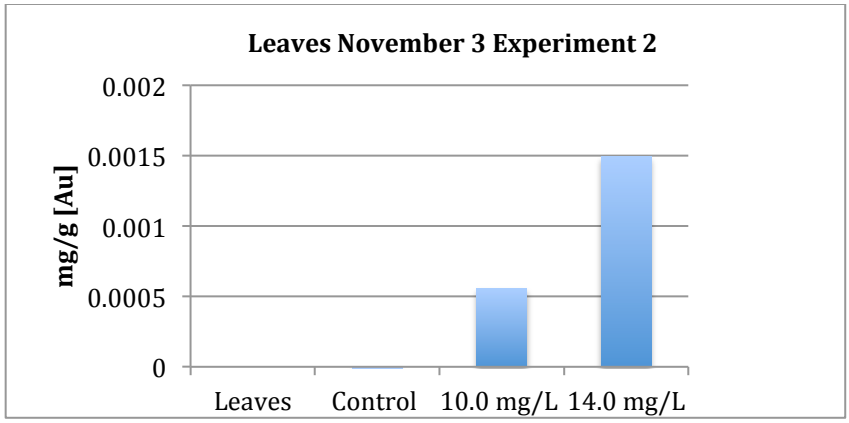

Figure A-11: Leaf tissue ICP-MS data that was run on Nov. 3, 2014.

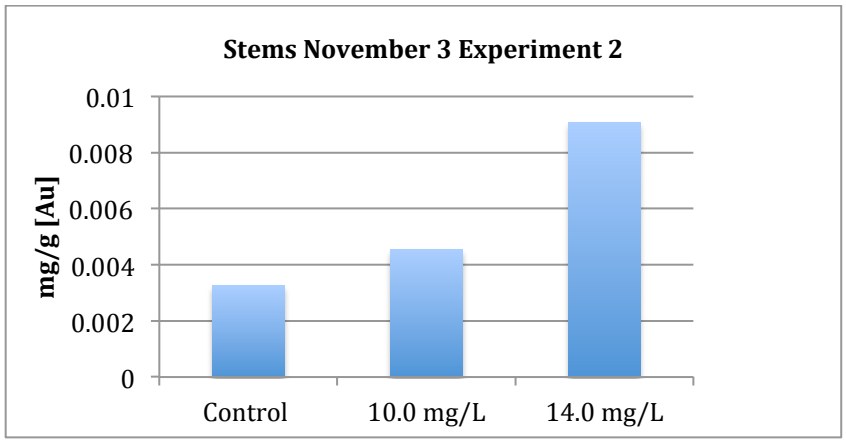

Figure A-12: Individual ICP-MS stem tissue data from experiment 3 that was run on Nov. 3, 2014.

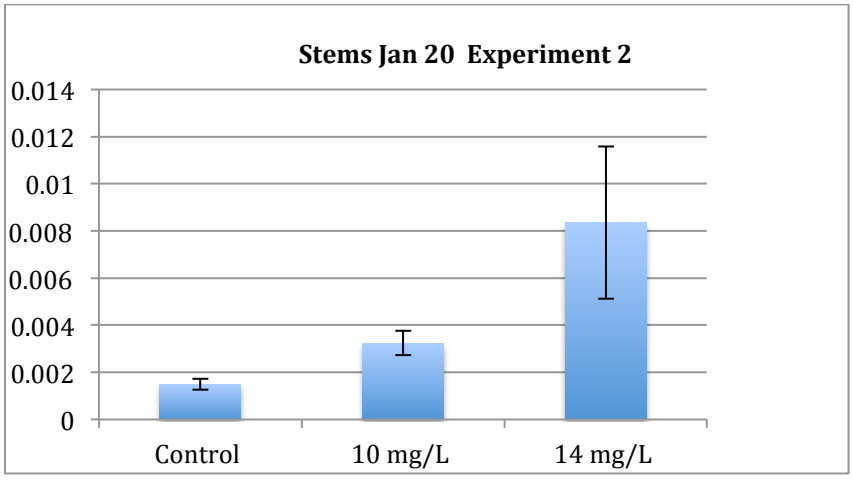

Figure A-13: ICP-MS results from stem tissue in Experiment 2 measure on January 20, 2015.

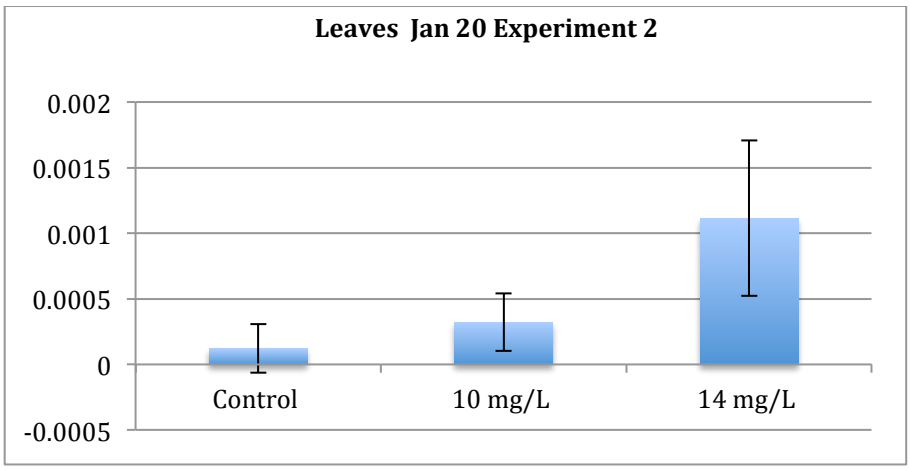

Figure A-14: Individual ICP-MS values for Leaves that was measured on January 20, 2015.

Table A-1: Comparison of solution standards throughout all ICP-MS runs. All show similar Au/Re standards throughout the experiment.

	19-Feb-15	20-Jan-15	17-Dec-14	3-Nov-14	12-Sep-14
	Au/Re	Au/Re	Au/Re	Au/Re	Au/Re
0 PPB AU		0.00			0.00
0.5 PPB	0.04	0.02	0.03	0.03	0.02
5 PPB AU	0.21	0.20	0.20	0.19	0.20
20 PPB AU	0.80	0.80	0.80		
50 PPB AU	1.99	1.99	2.04	1.89	2.14
Slope	5.02E-05	5.02E-05	4.92E-05	5.30E-05	4.66E-05

References

Alanazi, F. K., Radwan, A. A., & Alsarra, I. A. (2010). Biopharmaceutical applications of nanogold. *Saudi Pharmaceutical Journal : SPJ, 18*(4), 179-193. doi: 10.1016/j.jsps.2010.07.002

Albersheim, P. (2011). *Plant Cell Walls: From Chemistry to Biology.* . New York, USA: Garland Science.

Arruda, S. C., Silva, A. L., Galazzi, R. M., Azevedo, R. A., & Arruda, M. A. (2015). Nanoparticles applied to plant science: a review. *Talanta, 131*, 693-705. doi: 10.1016/j.talanta.2014.08.050

Arvizo, R., Bhattacharya, R., & Mukherjee, P. (2010). Gold nanoparticles: opportunities and challenges in nanomedicine. *Expert Opin Drug Deliv, 7*(6), 753-763. doi: 10.1517/17425241003777010

Bastus, N. G., Comenge, J., & Puntes, V. (2011). Kinetically controlled seeded growth synthesis of citrate-stabilized gold nanoparticles of up to 200 nm: size focusing versus Ostwald ripening. *Langmuir, 27*(17), 11098-11105. doi: 10.1021/la201938u

Berglund, D. R. (2011). Crops Vary in Their Tolerance to Frost. Retrieved from Winter Storm Information website: <http://www.ag.ndsu.edu/winterstorm/winter-storm-information-farm-and-ranch-information/farm-and-ranch-crops-general/crops-vary-in-their-tolerance-to-frost>

Blankendaal, M., Hodgson, R.H., Davis D.G., Hoerauf R.A., Shimabukuro R.H. (1972). *Growing Plants without Soil for Experimental Use*. Washington D.C. .

Burken, J. G., & Schnoor, J. L. (1998). Predictive relationships for uptake of organic contaminants by hybrid poplar trees. *Environ Sci Technol, 32*(21), 3379-3385.

Canesi, L., Ciacci, C., Fabbri, R., Marcomini, A., Pojana, G., & Gallo, G. (2012). Bivalve molluscs as a unique target group for nanoparticle toxicity. *Mar Environ Res, 76*, 16-21. doi: 10.1016/j.marenvres.2011.06.005

Carlson, R. B., F.A., Rolfe, G.L. (1974). The Effect of Heavy Metals on Plants *Environ Res*(10), 113-120.

Carpentier, A., Abreu, S., Trichet, M., & Satiat-Jeunemaitre, B. (2012). Microwaves and tea: new tools to process plant tissue for transmission electron microscopy. *Journal of microscopy, 247*(1), 94-105.

Carpita, N., Sabularse, D, Montezinos, Delmar, DP. (1979). Determination of the pore-size of cell-walls of living plant cells. *Science*(205), 1144-1147.

Chen, H., Seiber, J. N., & Hotze, M. (2014). ACS Select on nanotechnology in food and agriculture: a perspective on implications and applications. *J Agric Food Chem, 62*(6), 1209-1212. doi: 10.1021/jf5002588

Corredor, E., Testillano, P. S., Coronado, M.-J., González-Melendi, P., Fernández-Pacheco, R., Marquina, C., . . . Pérez-de-Luque, A. (2009). Nanoparticle penetration and transport in living pumpkin plants: in situ subcellular identification. *BMC plant biology, 9*(1), 45.

Crop Values 2013 Summary. (2014). USDA.

Deng, Y.-q., White, J. C., & Xing, B.-s. (2014). Interactions between engineered nanomaterials and agricultural crops: implications for food safety. *Journal of Zhejiang University SCIENCE A, 15*(8), 552-572. doi: 10.1631/jzus.A1400165

Eichert, T., Kurtz, A., Steiner, U., & Goldbach, H. E. (2008). Size exclusion limits and lateral heterogeneity of the stomatal foliar uptake pathway for aqueous solutes and water-suspended nanoparticles. *Physiologia Plantarum, 134*(1), 151-160. doi: 10.1111/j.1399-3054.2008.01135.x

Enustun, B. V., & Turkevich, J. (1963). Coagulation of Colloidal Gold. *Journal of the American Chemical Society, 85*(21), 3317-3328. doi: 10.1021/ja00904a001

Etxeberria, E., Gonzalez, P., & Pozueta, J. (2009). Evidence for two endocytic transport pathways in plant cells. *Plant Science, 177*(4), 341-348. doi: 10.1016/j.plantsci.2009.06.014

Etxeberria, E., Pozueta-Romero, J. Fernandez, E. (2012). *Fluid Phase Endocytosis in Plants* J. Samaj (Ed.) *Endocytosis in Plants*

Etxeberria, E. G., P. . (2006). Fluid Phase Endocytic Uptake of Artificial Nano-Fluorescent Quantum Dots by Sycamore Cultures. *Plant Signaling and Behavior, 1*(3), 196-200.

Faraday, M. (1857). The Bakerian Lecture: Experimental Relations of Gold (and other Metals to light). *Philosophical Transaction of Royal Society of London, 147*, 145-181.

Giljohann, D. A., Seferos, D. S., Daniel, W. L., Massich, M. D., Patel, P. C., & Mirkin, C. A. (2010). Gold nanoparticles for biology and medicine. *Angew Chem Int Ed Engl, 49*(19), 3280-3294. doi: 10.1002/anie.200904359

Gole, A. M., J. . (2005). Plyelectrolyte-Coated Gold Nanorods: Synthesis, Characterization and Immobilization. *Chem. Mater., 17*(6), 1325-1330.

Gonzalez-Melendi, P., Fernandez-Pacheco, R., Coronado, M. J., Corredor, E., Testillano, P. S., Risueno, M. C., . . . Perez-de-Luque, A. (2008). Nanoparticles as smart treatment-delivery systems in plants: assessment of different techniques of microscopy for their visualization in plant tissues. *Ann Bot, 101*(1), 187-195. doi: 10.1093/aob/mcm283

Hawthorne, J., Musante, C., Sinha, S. K., & White, J. C. (2012). Accumulation and phytotoxicity of engineered nanoparticles to Cucurbita pepo. *International Journal of Phytoremediation, 14*(4), 429-442.

Huang, X., Neretina, S., El-Sayed, M. . (2009). Gold Nanorods: From Synthesis and Properties to Biological and Biomedical Applications. *Advanced Materials, 21*, 4880-4910.

Irani NG, D. R. S., Mylle E, Van Den Begin J, Schneider-Pizon´ J, Hniliková J, Šíša M, Buyst D, Vilarrasa-Blasi J, Szatmári AM, Van Damme D, Mishev K, Codreanu MC, Kohout L, Strnad M, Caño-Delgado AI, Friml J, Madder A, Russinova E. (2012). Fluorescent castasterone reveals BRI1 signaling from the plasma membrane. *Nat Chem Biol, 8*, 583-589.

Iravani, S. (2011). Green synthesis of metal nanoparticles using plants. *Green Chemistry, 13*(10), 2638. doi: 10.1039/c1gc15386b

Judy, J. D., Unrine, J. M., & Bertsch, P. M. (2010). Evidence for biomagnification of gold nanoparticles within a terrestrial food chain. *Environ Sci Technol, 45*(2), 776-781.

Karnovsky, M. J. (1965). A formaldehyde-glutaraldehyde fixative of high osmolarity for use in electron microscopy. *J. cell Biol, 27*.

Kato, K. (1967). The osmium tetroxide procedure for light and electron microscopy of ABS plastics. *Polymer Engineering & Science, 7*(1), 38-39.

Keller, A. W., Hongtao, Zhou, D, Lenihan, H., Cherr, G., Cardinale, B., Miller, R., Ji, Z. . (2010). Stability and Aggregation of Metal Oxide Nanoparticle in Natural Aqueous Matrices. *Environ. Sci. Technol.*(44), 1963-1967.

Khodakovskaya M.; de Silva M.; Biris, A. D., E.; Villagarcia H. (2012). Carbon Nanotubes Induce Growth Enhancement of Tobacco Cells 2. *ACS Nano, 6*(3), 2129-2135.

Khodakovskaya, M. V., de Silva, K., Biris, A. S., Dervishi, E., & Villagarcia, H. (2012). Carbon Nanotubes Induce Growth Enhancement of Tobacco Cells. *ACS Nano, 6*(3), 2128-2135. doi: 10.1021/nn204643g

Kim, J. H., Oh, Y., Yoon, H., Hwang, I., & Chang, Y. S. (2015). Iron Nanoparticle-Induced Activation of Plasma Membrane H(+)-ATPase Promotes Stomatal Opening in Arabidopsis thaliana. *Environ Sci Technol, 49*(2), 1113-1119. doi: 10.1021/es504375t

Klaine, S. J., Alvarez, P. J. J., Batley, G. E., Fernandes, T. F., Handy, R. D., Lyon, D. Y., . . . Lead, J. R. (2008). Nanomaterials in the environment: behavior, fate, bioavailability, and effects. *Environmental Toxicology and Chemistry, 27*(9), 1825-1851.

Kumar, V., & Yadav, S. K. (2009). Plant-mediated synthesis of silver and gold nanoparticles and their applications. *Journal of Chemical Technology & Biotechnology, 84*(2), 151-157. doi: 10.1002/jctb.2023

Kurepa, J., Paunesku, T., Vogt, S., Arora, H., Rabatic, B. M., Lu, J., . . . Smalle, J. A. (2010). Uptake and distribution of ultrasmall anatase TiO2 Alizarin red S nanoconjugates in Arabidopsis thaliana. *Nano Lett, 10*(7), 2296-2302. doi: 10.1021/nl903518f

Larue, C., Laurette, J., Herlin-Boime, N., Khodja, H., Fayard, B., Flank, A.-M., Carriere, M. (2012). Accumulation, translocation and impact of TiO2 nanoparticles in wheat (Triticum aestivum spp.): Influence of diameter and crystal phase. *Science of The Total Environment, 431*(0), 197-208. doi: <http://dx.doi.org/10.1016/j.scitotenv.2012.04.073>

Lee, W. A., Y., Yoon, H., Kweon, H. (2008). Bioavailability of copper nanoparticles to the terrestrial plants Mung Bean(Phaseolus Radiatus) and wheat (Triticum aestivum): Plant agar test for water-insoluble nanoparticles. *Envriron Toxicol, 27*(9), 1915-1921.

Lin, D., & Xing, B. (2007). Phytotoxicity of nanoparticles: inhibition of seed germination and root growth. *Environ Pollut, 150*(2), 243-250. doi: 10.1016/j.envpol.2007.01.016

Lin, S., Reppert, J., Hu, Q., Hudson, J. S., Reid, M. L., Ratnikova, T. A., . . . Ke, P. C. (2009). Uptake, translocation, and transmission of carbon nanomaterials in rice plants. *Small, 5*(10), 1128-1132. doi: 10.1002/smll.200801556

Liu, Q. C., B.; Wang Q.; Shi X.; Xiao, Z.; Lin J.; Fang X. (2009). CNTS as molecular transport for walled plant cells. *Nano Lett, 9*(3), 1007-1010.

Mahmood, T. M. A., S., Tajammul Hussain, S. Aamir, S. . (2012). Metallic phytoremediation and extraction of nanoparticles. *International Journal of Physical Sciences, 7*(46), 6105-6116. doi: 10.5897/IJPS12.605

McCann, M., Wlls, B, Roberts, K. . (1990). Direct Visualization of cross-links in the primary plant cell wall. *J Cell Sci*(96), 323-334.

McFarland, A. D., Van Duyne R.P., Godwin, H.A. (2004). Color my Nanoworld. *J. Chem. Educ, 81*(544A).

Miralles, P., Church, T. L., & Harris, A. T. (2012). Toxicity, Uptake, and Translocation of Engineered Nanomaterials in Vascular plants. *Environ Sci Technol, 46*(17), 9224-9239. doi: 10.1021/es202995d

Moradi, N. (2014). *Uptake, Translocation and Toxicity of Gold Nanorods in Maize.* (Masters), The University of Iowa.

Navarro, E., Baun, A., Behra, R., Hartmann, N. B., Filser, J., Miao, A.-J., . . . Sigg, L. (2008). Environmental behavior and ecotoxicity of engineered nanoparticles to algae, plants, and fungi. *Ecotoxicology, 17*(5), 372-386.

Onelli, E., Prescianotto-Baschong, C., Caccianiga, M., & Moscatelli, A. (2008). Clathrin-dependent and independent endocytic pathways in tobacco protoplasts revealed by labelling with charged nanogold. *J Exp Bot, 59*(11), 3051-3068. doi: 10.1093/jxb/ern154

Perez-Juste, J. P.-S., I. Liz Marzan, L., Mulvaney, P. (2005). Gold nanorods: Synthesis, characterization and applications. *Coordination Chemistry Review, 249*(1870-1901).

Pitcairn, I. K., Warwick, P. E., Milton, J. A., & Teagle, D. A. H. (2006). Method for ultra-low-level analysis of gold in rocks. *Analytical chemistry, 78*(4), 1290-1295.

Proseus, T. E., & Boyer, J. S. (2005). Turgor pressure moves polysaccharides into growing cell walls of Chara corallina. *Ann Bot, 95*(6), 967-979. doi: 10.1093/aob/mci113

Ranjan, S. D., N., Charaborty, A. Samuel, S, Ramalingam, C, Shanker, R, Kumar, A. (2014). Nanoscience and nanotechnologies in food industry: opportunities and research trends. *Journal of nanoparticle research, 16*(2464), 1-23.

Rico, C. M., Majumdar, S., Duarte-Gardea, M., Peralta-Videa, J. R., & Gardea-Torresdey, J. L. (2011). Interaction of nanoparticles with edible plants and their possible implications in the food chain. *J Agric Food Chem, 59*(8), 3485-3498. doi: 10.1021/jf104517j

Roco, M. C. (2011). The long view of nanotechnology development: the National Nanotechnology Initiative at 10 years. *Journal of nanoparticle research, 13*(2), 427-445. doi: 10.1007/s11051-010-0192-z

Rubbo S.D.; Russinova, E. (2012). Receptor-Mediated Endocytosis in Plants. In J. Samaj (Ed.), *Endocytosis in Plants* (pp. 151-160). Berlin Heidelberg: Springer.

Seeger, E. M., Baun, A., Kästner, M., & Trapp, S. (2008). Insignificant acute toxicity of TiO2 nanoparticles to willow trees. *Journal of Soils and Sediments, 9*(1), 46-53. doi: 10.1007/s11368-008-0034-0

Serag, M., & Kaji, N. G., C.; Okamoto Y.; Terasaka, K.; Jabasini, M.; Manabu, T.; Mizukami, H.; Bianco, A. Baba, Y. . (2011). Trafficking and Subcellular Localization of Multiwalled Carbon Nanotubes in Plant Cells copy. *ACS Nano, 5*(1), 493-499.

Seth, C. S., Misra, V., Singh, R. R., & Zolla, L. (2011). EDTA-enhanced lead phytoremediation in sunflower (Helianthus annuus L.) hydroponic culture. *Plant and Soil, 347*(1-2), 231-242. doi: 10.1007/s11104-011-0841-8

Shen, C. X., Zhang, Q. F., Li, J., Bi, F. C., & Yao, N. (2010). Induction of programmed cell death in Arabidopsis and rice by single-wall carbon nanotubes. *Am J Bot, 97*(10), 1602-1609. doi: 10.3732/ajb.1000073

Singh, S., & Sinha, S. (2004). Scanning electron microscopic studies and growth response of the plants of Helianthus annuus L. grown on tannery sludge amended soil. *Environ Int, 30*(3), 389-395. doi: 10.1016/j.envint.2003.09.006

Spurr, A. R. (1969). A low-viscosity epoxy resin embedding medium for electron microscopy. *Journal of ultrastructure research, 26*(1), 31-43.

Spurr, A. R., & Harris, W. M. (1968). Ultrastructure of chloroplasts and chromoplasts in Capsicum annuum. I. Thylakoid membrane changes during fruit ripening. *Am J Bot*, 1210-1224.

Sunflower Statistics. (2015, January 2015). March 2015, from http://www.sunflowernsa.com/stats/

Terzakis, J. A. (1968). Uranyl acetate, a stain and a fixative. *Journal of ultrastructure research, 22*(1), 168-184.

Thakkar, K. N., Mhatre, S. S., & Parikh, R. Y. (2010). Biological synthesis of metallic nanoparticles. *Nanomedicine: Nanotechnology, Biology and Medicine, 6*(2), 257-262.

Torney, F., Trewyn, B. G., Lin, V. S., & Wang, K. (2007). Mesoporous silica nanoparticles deliver DNA and chemicals into plants. *Nat Nanotechnol, 2*(5), 295-300. doi: 10.1038/nnano.2007.108

Tyerman, S. D., Niemietz, C. M., & Bramley, H. (2002). Plant aquaporins: multifunctional water and solute channels with expanding roles. *Plant, Cell & Environment, 25*(2), 173-194. doi: 10.1046/j.0016-8025.2001.00791.x

Verma, A., & Stellacci, F. (2010). Effect of surface properties on nanoparticle-cell interactions. *Small, 6*(1), 12-21. doi: 10.1002/smll.200901158

Verma, A., Uzun, O., Hu, Y., Hu, Y., Han, H. S., Watson, N., Stellacci, F. (2008). Surface-structure-regulated cell-membrane penetration by monolayer-protected nanoparticles. *Nat Mater, 7*(7), 588-595. doi: 10.1038/nmat2202

Wang, J., Koo, Y., Alexander, A., Yang, Y., Westerhof, S., Zhang, Q., . . . Alvarez, P. J. J. (2013). Phytostimulation of poplars and Arabidopsis exposed to silver nanoparticles and Ag+ at sublethal concentrations. *Environ Sci Technol, 47*(10), 5442-5449.

Wild, E., & Jones, K. C. (2009). Novel method for the direct visualization of in vivo nanomaterials and chemical interactions in plants. *Environmental science & technology, 43*(14), 5290-5294.

Wilson-Corral, V. R.-L., M. Lopez-Perez, J., Arenas-Vargas M., Anderson, C. . (2010). *Gold phytomining in arid and semiarid soils*. 19th World Congress of Soil Science, Soil Solutions for a Changing World.

Xia, B., Dong, C., Zhang, W., Lu, Y., Chen, J., & Shi, J. (2013). Highly efficient uptake of ultrafine mesoporous silica nanoparticles with excellent biocompatibility by Liriodendron hybrid suspension cells. *Sci China Life Sci, 56*(1), 82-89. doi: 10.1007/s11427-012-4422-8

Zhang, M., & Akbulut, M. (2011). Adsorption, desorption, and removal of polymeric nanomedicine on and from cellulose surfaces: effect of size. *Langmuir, 27*(20), 12550-12559.